How microbial communities shape peatland carbon dynamics: New insights and implications

Etienne Richy, Pedro Cabello-Yeves, Felipe Hernandes-Coutinho, Francisco Rodriguez-Valera, Iván González-Álvarez, Laure Gandois, François Rigal, Béatrice Lauga

▶ **To cite this version:**

Etienne Richy, Pedro Cabello-Yeves, Felipe Hernandes-Coutinho, Francisco Rodriguez-Valera, Iván González-Álvarez, et al.. How microbial communities shape peatland carbon dynamics: New insights and implications. Soil Biology and Biochemistry, 2024, 191 (7), pp.109345. 10.1016/j.soilbio.2024.109345 . hal-04741789

HAL Id: hal-04741789
https://hal.science/hal-04741789v1

Submitted on 15 Nov 2024

HAL is a multi-disciplinary open access archive for the deposit and dissemination of scientific research documents, whether they are published or not. The documents may come from teaching and research institutions in France or abroad, or from public or private research centers.

L'archive ouverte pluridisciplinaire **HAL**, est destinée au dépôt et à la diffusion de documents scientifiques de niveau recherche, publiés ou non, émanant des établissements d'enseignement et de recherche français ou étrangers, des laboratoires publics ou privés.

Distributed under a Creative Commons Attribution - NonCommercial - ShareAlike 4.0 International License

Soil Biology and Biochemistry 191 (2024) 109345

Contents lists available at ScienceDirect

Soil Biology and Biochemistry

journal homepage: www.elsevier.com/locate/soilbio

How microbial communities shape peatland carbon dynamics: New insights and implications

Etienne Richy [a,**], Pedro J. Cabello-Yeves [b,e,f], Felipe Hernandes-Coutinho [b,d], Francisco Rodriguez-Valera [b], Iván González-Álvarez [a], Laure Gandois [c], François Rigal [a], Béatrice Lauga [a,*]

[a] Universite de Pau et des Pays de l'Adour, E2S UPPA, CNRS, IPREM, Pau, France
[b] Evolutionary Genomics Group, Departamento de Producción Vegetal y Microbiología, Universidad Miguel, Hernández, San Juan de Alicante, Alicante, Spain
[c] Laboratoire Écologie Fonctionnelle et Environnement, Université de Toulouse, CNRS, Toulouse, France
[d] Current Affiliation: Department of Marine Biology and Oceanography, Institute of Marine Sciences (ICM), CSIC, Barcelona, Spain
[e] Cavanilles Institute of Biodiversity and Evolutionary Biology, University of Valencia, E-46980, Paterna, Valencia, Spain
[f] Current Affiliation: School of Life Sciences, University of Warwick, Coventry, CV4 7AL, UK

ARTICLE INFO

Keywords:
Peat
Metagenomics
Microbial diversity
Microbial activities
Viruses
C accumulation
Ecosystem functioning

ABSTRACT

Peatlands are considered the most efficient ecosystem for long-term storage of atmospheric carbon (C). However, reasons for variations in C accumulation within peatlands remain largely unexplained. Using a comprehensive multi-level approach combining soil-atmosphere C exchanges, microbial extracellular enzyme activities, and genome-resolved cellular and viral metagenomics, we endeavored to decipher the microbial determinants and their role in C dynamics in the bog and fen of a European peatland. Overall, the bog exhibited a higher C content and dissolved organic carbon concentration. Despite contrasting geochemical conditions, these differences were not explained by environmental parameters nor the vegetation. Metagenomic analyses revealed varying microbial community composition, the bog being less diverse and dominated by Acidobacteriota and the fen comprising five predominant phyla (Crenarcheota, Chloroflexota, Proteobacteria, Desulfobacterota and Acidobacteriota). Both bog and fen microbial communities were stable between spring and summer. Yet, similar CO_2 emissions were recorded in both bog and fen, along with similar organic matter (OM) decomposition microbial activities and potential. Ultimately, the bog harbored significantly more viruses than the fen. Most intriguingly, these viruses were predicted to target Acidobacteriota, the phyla displaying the highest OM-degrading capacity in the bog. By impairing the activity of the dominant players in OM degradation, viruses might have a significant role in C dynamics in the bog over time. In addition, we propose that low microbial diversity limited cross-feeding opportunities in the bog, further limiting C degradation. Taken together, this study deciphers the role of microbial communities driving C accumulation in peatlands and, consequently, peatland ecosystem functioning.

1. Introduction

Peatlands are waterlogged and predominantly anoxic environments, in which plant production is favored over microbial degradation, leading to an accumulation of carbon over time (Rydin et al., 2006). Covering only 4.632 million km^2 of the total land mass (~3 %), peatlands store about one third of the total carbon (C) contained in soils (Xu et al., 2018; Yu et al., 2011), making them the most efficient ecosystem for long-term storage of atmospheric carbon. However, C accumulation rates can vary greatly between peatland types. Evidence shows that bogs tend to accumulate more C than fens (Thormann et al., 1999; Turunen et al., 2002; Watmough et al., 2022). Fens and bogs are the two major forms of northern peatlands which represent 91 % of peatlands worldwide (Yu et al., 2010). Bogs receive water and nutrients from rainfall, are nutrient poor, and acidic (pH < 5.5). They are dominated by *Sphagnum* spp., which are slowly decomposed due to the presence of

* Corresponding author.
** Corresponding author.
E-mail addresses: etiennerichy.art@gmail.com (E. Richy), beatrice.lauga@univ-pau.fr (B. Lauga).

https://doi.org/10.1016/j.soilbio.2024.109345
Received 3 November 2023; Received in revised form 30 January 2024; Accepted 1 February 2024
Available online 2 February 2024
0038-0717/© 2024 Published by Elsevier Ltd.

antimicrobial aromatic substances (e.g., polyphenols) (Bengtsson et al., 2018; Lang et al., 2009; Verhoeven and Liefveld, 1997). Fens are characterized by higher pH (pH > 5.5), dominated by more easily decomposable litter from sedges, grasses, and shrubs, and fed by both precipitation and groundwater which, in turn, lead to higher nutrient concentrations (Joosten and Clarke, 2002).

Ecological gradients, trophic status, vegetation cover and hydrology are associated with the variation in C dynamics between bogs and fens, in which microbial communities play a critical role. Bogs are commonly characterized by low microbial organic matter (OM) degradation rates (Bragazza et al., 2007; Lin et al., 2012; Preston et al., 2012), carbon dioxide (CO_2) production and methane (CH_4) emissions (Abdalla et al., 2016; Danevčič et al., 2010; Webster et al., 2018) compared to fens. However, recent findings (Hoyos-Santillan et al., 2018; McGivern et al., 2021; Turetsky, 2003; Urbanová and Hájek, 2021) have challenged the view that inhibitory compounds and low nutrient concentrations – two common features of bogs – hinder OM degradation in peatlands (Abdalla et al., 2016; Dorrepaal et al., 2005; Webster et al., 2018). Consequently, our understanding of how biotic interactions influence C accumulation rates in bogs and fens remains limited. In the context of climate change, which could impair C balance in peatlands (Loisel et al., 2021), the need to decipher the mechanisms underlying C accumulation in these ecosystems – including the microbial determinants and their role in belowground C dynamics – has become critical. A comprehensive overview of C dynamics in peatlands should also take into consideration the specificity of bogs and fens (Wu and Roulet, 2014).

Given their contrasting environmental features, we first hypothesize that bogs and fens should exhibit different prokaryotic communities (Finn et al., 2020; Seward et al., 2020; St. James et al., 2021). We anticipate that the difference in C dynamics between bogs and fens should be reflected in varying capacities for OM degradation, including organic polymer hydrolysis, fermentation, methanogenesis and methanotrophy (Drake et al., 2009; Horn et al., 2003; Woodcroft et al., 2018; Ye et al., 2012). As wetland ecosystems harbor exceptional viral abundance (Williamson et al., 2017), we also hypothesize that viruses play a role in peatland C cycle. Viruses can negatively or positively influence OM degradation (Dalcin Martins et al., 2018) either by killing OM-recycling microorganisms or by manipulating the metabolisms of their hosts through the expression of auxiliary metabolic genes (AMGs) (Chen et al., 2020). To date, the role of viruses in C cycling in wetlands have mainly been examined in permafrost peatlands (Emerson et al., 2018; Trubl et al., 2018, 2021), despite representing less than half of the total peatland surface area (Hugelius et al., 2020). As permafrost soils differ in many aspects from temperate peatlands (Jansson and Taş, 2014), it is crucial to examine also their role in bogs and fens C cycling to gain a more comprehensive overview of microbial drivers of C dynamics in peatlands.

Herein, we focus on a single mountainous peatland located in the Pyrenees (Bernadouze in Ariège, France) to disentangle microbial determinants over C dynamics along a bog to fen gradient. By comparing bog and fen within the same system, our study model overcomes the inherent confounding factors (e.g., temperature, precipitation, solar radiation) that could come into play when such a comparison is undertaken at large spatial scales. To obtain a representative picture of C dynamics of the peatland, we quantified dissolved organic carbon (DOC) and organic C concentrations, C densities and estimated CO_2 and CH_4 instantaneous flux in both bog and fen sites. A total of 24 samples were collected (bog and fen at three different depths) during two seasons (spring and summer). We have adopted a comprehensive multi-level approach to investigate the full range of microbiological processes involved in C dynamics. We thus performed enzymatic assays of five key hydrolase enzymes to assess microbial OM degradation, identify the key players involved in this process by analyzing the metabolic capacity of 290 unique bacterial and archaeal metagenome-assembled genomes (MAGs). We studied environmental determinants (abiotic) on microbial diversity, composition, and activities (biotic). Lastly, the contribution of viruses to peatland functioning was assessed by ecogenomic approaches, in which the distribution and dynamics of viruses were investigated, their hosts predicted and the putative AMGs encoded by the viruses characterized.

2. Materials and methods

2.1. Study site description and sample collection

Peat samples were collected at Bernadouze (42.80247 N, 1.42333 E), a mountainous peatland located at an altitude of 1344 m in the central part of the Pyrenees (Fig. 1A). Bernadouze was formed from a post-glacial lake, where a marsh existed for 10,000 years. This peatland covers an area of 4.7 ha, a 1.4 km^2 watershed, mainly composed of limestone (Jalut et al., 1982; Reille, 1990). The mean annual temperature recorded for the years 2015–2018 was 7.9 ± 0.3 °C and the mean annual precipitation was 1797 ± 265 mm. Sub-zero temperatures and snowfalls are frequently recorded at Bernadouze from mid-October to mid-May (Rosset et al., 2019). The Bernadouze peatland harbors a typical peatland vegetation cover, with bogs mainly dominated by sphagnum mosses and fens by vascular plants (Joosten and Clarke, 2002).

The sampling campaigns dedicated to microbial ecogenomics were carried out during the growing season (June 12 and 13, 2018), and at the end of summer (September 4 and 5, 2018). As the fen is largely predominant at Bernadouze (Fig. 1A), we over-sampled the fen compared to the bog. We collected samples from two sites in the fen and from one site in the bog. To better encompass the peatland's heterogeneity, we collected samples from both hummock and hollow at each site. For the hummocks, we used a 1 m^2 quadrat and collected three 1-m-deep cores (triplicate) using a Russian-type peat corer (5 cm × 50 cm). As the corer was 50 cm long, each core was the result of two consecutive core samplings (one replicate) to reach the depth of 1 m. Samples were collected from each core at three different depths: the surface (0–15 cm), the middle (35–50 cm) and the bottom of the core (85–100 cm). For the hollow, triplicates were collected at ~30 cm from the edge of the hollow, maintaining a 1 m distance between each core sampling. Only surface samples were collected for this microform. Each sample was subsampled in the field immediately after the core sampling and transferred directly to a liquid nitrogen container for molecular analysis. These subsamples were stored at −80 °C in the lab. A second subsample was taken in the field immediately after the coring to measure the pH using Multiparameter MultiLine WTW® 3510 (Sentix 940 sensor). The remaining triplicates were pooled and mixed into a plastic bag (conserved at −20 °C) for further biogeochemical analyses and enzyme activity assays. Finally, we used a piezometer to record the water table (WT) depth the following day at each sampling site. The WT depth varied between 0 and -26 cm on average, regardless of the season (Wilcoxon, $p = 0.803$). Considering that the average peat depth of Bernadouze has been estimated at 2 m (Jalut et al., 1982; Reille, 1990), this result indicated prevalent anoxic conditions in the peatland.

2.2. Measuring geochemical parameters

Peat organic carbon (C content) and total nitrogen (N) were determined using a FLASH 2000 ThermoFisher™ elemental analyzer on samples dried during 24 h at 80 °C in an oven. Nutrient (i.e. NO_2, NO_3, SO_4^{2-}, NH_4^+, PO_4^{3-}) and DOC concentrations were analyzed from the water extracted samples. Briefly, 30 g of peat were added to 150 mL of Milli-Q ultra-pure water and agitated for one night at 150 rpm and 20 °C (Jones and Willett, 2006). Using a filter unit, four filtrations were carried out, including one with a Ø 80 µm nylon filter cloth, a second with a GF/A filter, a third with a GF/F filter and a final one with a 0.22 µm cellulose acetate filter. The nutrients were quantified by High-Performance Ion Chromatography (Dionex Ics-5000+ [anions]; Dionex DX-120 [cations]). Reference material included ION-915 and

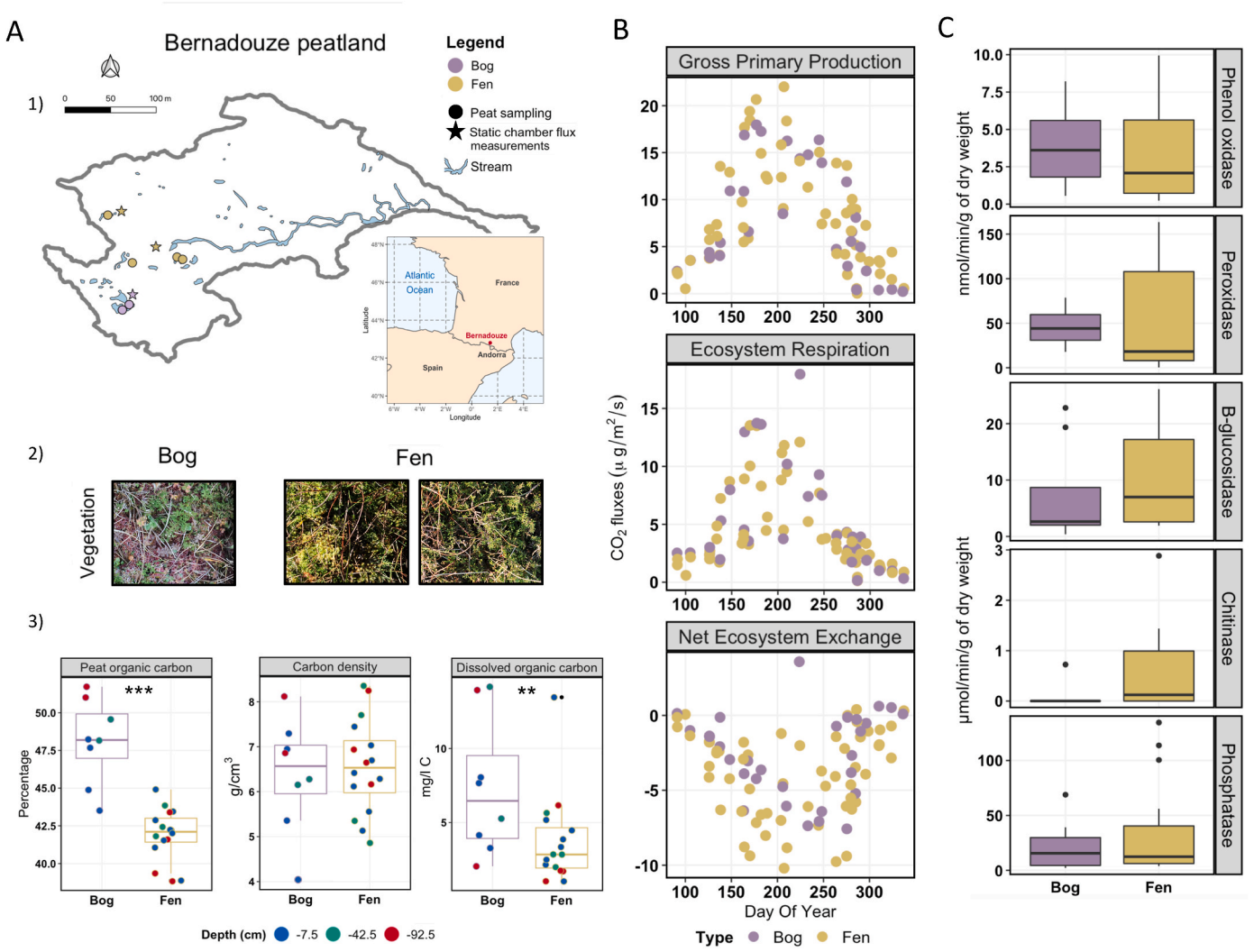

Fig. 1. Location of the Bernadouze peatland and carbon dynamics (peat organic carbon, dissolved organic carbon, atmospheric carbon fluxes and microbial enzymatic activities related to OM degradation). A. (1) Location of the Bernadouze peatland and sampling sites. The dots represent the locations of peat samplings and the stars the location of static chamber flux measurements. Purple and yellow color code indicates the bog and fen sites respectively. (2) Representative vegetation covers of the bog and the fen. (3) Box plots of peat organic carbon and dissolved organic carbon concentration, with n = 8 for bog and n = 16 for fen. Stars indicate the level of significance (** if p <0.01 and *** if p <0.001). B. Atmospheric carbon fluxes over six-year period. Gross Primary Production (GPP), Ecosystem Respiration (ER) and Net Ecosystem Exchange (NEE), measured in the bog (30 measures across 6 years) and the fen (57 measures across 6 years) using a static chamber flux. No significant variation (p > 0.05) between bog and fen were detected (Table S2). C. Comparison of enzymatic activities involved in the degradation of organic matter between bog (n = 8) and fen (n = 16). No significant variation (p > 0.05) between bog and fen were detected (Table S2).

ION 96.4 (Environment and Climate Change Canada, Canada). The DOC concentration was analyzed from the filtered samples acidified to pH 2, using a TOC-5000A analyzer (Shimadzu, Japan).

Soluble polyphenols were also estimated from the water extracts. Briefly, 30 g of peat were added to 150 mL of Milli-Q ultra-pure water and agitated for 1 h. Using a 96-well microplate, 200 µL of this extract were mixed with 10 µL of 2 M of Folin-Ciocalteu reagent and 30 µL of Na_2CO_3 (100 $g.L^{-1}$). After 30 min of incubation at 40 °C, the absorbance wavelength was measured at 765 nm using a Synergy HTX Multi-Mode Reader machine. The standard curve was calculated using gallic acid at concentrations of 0, 5, 10, 20, 30, 40, 50 and 60 $mg.L^{-1}$. The phenolic content is expressed as a gallic acid equivalent, in milligrams per gram ($mg.g^{-1}$) of dry weight of peat.

Total polyphenols were also extracted. A solution composed of methanol, H_2O and HCl (75/24.5/0.5) was added to fresh peat, maintaining a 1/100 ratio (w/v). Samples were agitated in the dark for 2 h at 160 rpm and 35 °C and further centrifuged at 5000 rpm for 10 min at 20 °C. Then, the peat extract was diluted with water, maintaining a 1/10 ratio (v/v), and added to 10 µL of 2 M Folin-Ciocalteu reagent mixed and incubate for 2 min. Next, 30 µL of Na_2CO_3 (100 $g.L^{-1}$) were added and incubated for 2 h at 20 °C. The absorbance wavelength was measured at 765 nm using a Synergy HTX Multi-Mode Reader machine. The standard curve was calculated using gallic acid at concentrations of 0, 50, 100, 150, 250 and 500 $mg.L^{-1}$ diluted at 1/80. The phenolic content is expressed as a gallic acid equivalent, in $mg.g^{-1}$ of dry weight of peat.

2.3. *Measuring fluxes using static chambers*

During snow-free periods, soil to atmosphere greenhouse gas (GHG) exchanges were measured monthly using static chambers. Collars had been installed 1 month prior to the first measurements in May 2016. For each station, measurements were first performed using a transparent acrylic chamber (30 cm diameter and 30 cm high) to measure the NEE (net ecosystem exchange). The measurement was then repeated in the dark by covering the chamber with an opaque aluminum cover to measure the ER (ecosystem respiration). Changes in CO_2 and CH_4

concentrations within the chamber headspace were monitored respectively using a CARBOCAP® GMP 343 CO_2 probe (VAISALA) placed at the top of the chamber for CO_2 and a LI-COR LI-7810 analyzer connected to the chamber for CH_4.

CO_2 and CH_4 fluxes were then calculated from the linear regression of the concentrations within the chamber over time, using the following equation:

$$F_{co_2,CH_4} = \frac{d_{CO_2,CH_4}}{dt} * \frac{h}{1000} * \frac{Pa}{R*Ta}$$

where F is the CO_2 or CH_4 flux (μmol·m^{-2}·s^{-1}); $d_{CO_2,\ CH_4}$/dt is the variation in gas concentrations within the chamber as a function of time (ppm s^{-1}); h is the total headspace height (chamber + soil collar; mm); Pa is the atmospheric pressure (J m^{-3}); R is the ideal gas constant of 8.3144621 (J K^{-1} mol^{-1}); and Ta is the air temperature in the chamber (K). Finally, the gross primary production (GPP) was calculated as GPP = ER - 1*NEE.

2.4. Enzymatic activity assays

Microbial depolymerization activities of phenolic and lignin-type compounds were quantified through phenol oxidase (laccase) and peroxidase enzymatic activities, respectively, using 2,2′-Azino-bis(3-Ethylbenzthiazoline-6-Sulfonic Acid) (ABTS) as a substrate. Briefly, 50 mL of acetate buffer (0.1 M, pH = 4) were mixed with 0.5 g of fresh peat. In a 96-well microplate, 200 μL of solution were mixed with 50 μL of ABTS (0.1 M), incubated in the dark for 15 min at 21 °C and agitated at 150 rpm. The peroxidase enzymatic activity was estimated using the same protocol, adding 10 μL of H_2O_2 (0.3 %) to the reaction. The reaction was stopped by centrifugation at 5700 rpm for 5 min at 21 °C. Fluorescence was measured at 420 nm in 150 μL of solution using a Synergy HTX Multi-Mode Reader machine. Both phenol oxidase and peroxidase are expressed in μmol.min^{-1}.g^{-1} of peat dry weight. Acid phosphate (phosphatase), chitinase and B-glucosidase enzymatic activities were quantified following the BSI Standards Publication DD ISO TS 22939:2010.

2.5. DNA extraction, sequencing, assembly and read analysis

Triplicates of the subsamples were pooled and homogenized in a mortar using a pestle under liquid nitrogen. The DNA extraction of the 24 subsamples was performed using the DNeasy PowerSoil kit following the manufacturer's instructions (MoBio Laboratories, UK). Library preparation (PCR-free libraries) and sequencing was performed using an Illumina NovaSeq 6000 platform producing 150 bp paired-end reads, at the University of Maryland School of Medicine (USA). A total of 0.6 Tb of metagenomic reads data (from 18 to 47 Gb per sample) were obtained. Prior to any analysis on metagenomic raw reads, we eliminated sequencing errors using Trimmomatic (v0.36) (Bolger et al., 2014) with the following parameters: PE, -phred33, ILLUMINACLIP:adapters.fa:2:30:10, LEADING:3, TRAILING:3, SLIDINGWINDOW:4:15, MINLEN:50. This process involved either removing reads with errors or trimming specific regions within the read sequences, such as low-quality regions or adapters. Next, the metagenomes were assembled independently using IDBA-UD (v1.1.1) (Peng et al., 2012) with the following parameters: mink, 60; maxk, 120; step, 10 -pre-correction. We obtained 14 Gbp of contiguous sequences, of which 3 Gbp (21.4 %) were >5 kb.

Two of the 24 metagenomes (hummock surface in bog and fen of summer sampling campaign) were also sequenced using Pacbio Sequel II 8M SMRT Cell Run (30-h movie). The library preparation (with size selection) and the sequencing were also performed at the University of Maryland School of Medicine (USA). The DNA extraction was performed using the DNeasy PowerSoil Pro kit with slight optimization to avoid DNA shearing (no vortex, gentle homogenizations). We used Trimmomatic (v0.36) to remove adapters and poor-quality raw reads, and sequences <1 kb were discarded. We performed a hybrid assembly using the corresponding paired-end Illumina metagenomes, with SPADes (v3.13.1) (Prjibelski et al., 2020) using the following parameters: -pacbio –only-assembler –careful. We obtained approximately 10 million reads per sample, with an average length of 7 kb. More than 14,000 sequences were >10 kb in length, with an average length of 23 kb (Table S1). The Pacbio data were used to assemble additional high-quality genomes only.

Unassembled 16S rRNA and 18S rRNA read fragments were obtained using USEARCH (v9.2) (Edgar, 2010) with RefSeq 16S and 18S rRNA genes as databases from December 2019 respectively, and then confirmed using ssu-align (v0.1.1) (Nawrocki and Eddy, 2010) on a subsampling of 10 million reads per sample. To provide a taxonomic classification (Cabello-Yeves et al., 2020), reads were mapped using BLASTn (v2.9.0) (Altschul et al., 1990) against the SILVA database v138 from December 2019 (Quast et al., 2012) using a maximum e-value of 1×10^{-5}. In total, we identified 44,012 16S rRNA and 2252 18S rRNA sequences representing 1834 ± 382 and 94 ± 95 sequences per sample respectively. Among the 18S rRNA sequences identified, 72 were fungal sequences, representing 3 ± 4 sequences per sample.

2.6. Estimating microbial abundance

qPCR was employed to estimate total prokaryote and fungal abundances. For prokaryotes, the 16S rRNA gene was amplified using the primer pairs 341F (5′-CCTACGGGAGGCAGCAG-3) (Muyzer et al., 1993) and 514R (5′-ATTCCGCGGCTGGCA-3′) (Lopez-Gutierrez et al., 2004), and a standardized commercial plasmid of *E. coli* (pk3) 16S rRNA gene (X80731.1) was used as a standard. For fungi, the 18S rRNA gene was amplified using the primer pairs nu-SSU-1196F (5′-GGAAACTCACCAGGTCCAGA-3) and nu-SSU-1536R (5′-ATTGCAATGCYCTATCC CCA-3′) (Borneman and Hartin, 2000). The primer set was validated on the peatland DNA extractions. An 18S standard was built from one of those PCR products after it has been purified using illustra GFXTM PCR DNA and a Gel Band Purification Kit (GE Healthcare) following the manufacturer's instructions and cloned using pGEM®-T Easy vector ligation (Promega). Transformation of the recombinant plasmid was performed using One ShotTM TOP10 Chemically Competent *E. coli* (Invitrogen) according to the manufacturer's protocol. After overnight incubation in LB Agar (Conda Pronadisa) supplemented with ampicillin (100 mg mL^{-1}), X-gal (20 mg mL^{-1}) and IPTG (200 mg mL^{-1}), colonies possessing the insert were replicated in an LB Broth medium (Conda Pronadisa) under the same ampicillin condition and incubated overnight. Plasmids were extracted using the QIAprep Spin Miniprep Kit (QIAGEN) according to the manufacturer's protocol and verified in agarose 1 % gel. The linearization of the final plasmid product was performed by enzymatic digestion with the *Pst*I enzyme (New England Biolabs) and then quantified using the Quant-iTTM PicoGreenTM dsDNA Assay Kit (Invitrogen). The plasmid insert was sequenced and analyzed using the NCBI "BLAST" analysis tool and matched at 99.70 % of identity (e-value: 2e- 163) with fungal sp. strain 2P1CQ1 (MH429421.1).

Each PCR reaction was set up in a 96-well plate using 10 μL Takyon™ No Rox SYBR® MasterMix dTTP Blue (Eurogentec)1x, 2 μL Forward/Revers primers, 1 μL of DNA sample and 4 μL of water (20 μL of total volume). qPCR was performed on a LightCycler® 480 96-Multiwell Plates instrument (Roche Diagnostics), with an initial denaturation and Takyon™ activation at 95 °C for 3 min, followed by 40 cycles of denaturation at 95 °C for 3 min, annealing at 60 °C for 30 s and extension time at 72 °c during 20 s for the 16S primer set and 40 s for the 18S primer set. The samples were run in triplicates, and qPCR plates included standard curves in duplicate and a negative control. Absolute copy number quantification was calculated by plotting Cycle threshold (Ct) values against the standard curve of a 10-fold dilution series of the plasmid copy number concentration. Microbial abundance was corrected by soil dry weight to normalize the copy number data set.

2.7. Genome binning, MAG quality assessment and annotation

MAGs were obtained using MetaBAT2 (v2.12.1) (Kang et al., 2019) and manual curation. Briefly, contigs longer than 5 kb (Illumina) and 10 kb (PacBio) were indexed aligned to short read sequences. Next, SAMtools (v1.10) was used to sort BAM files and each contig coverage depth was calculated using Bowtie2 (2.3.5) (Langmead and Salzberg, 2012). This information was used to apply binning by coverage (Metabat2). CheckM (v1.0.18) was used to assess completeness and contamination of each bin (Parks et al., 2015). We recovered a total of 515 genomic bins filtered by completeness (>50 %) and contamination (<5 %). To identify redundant genomes (dereplication), the average nucleotide identity (ANI) score was calculated using a cutoff ≥95 % and only non-redundant genomes with the highest quality scores or greatest overall sizes were kept. The taxonomic assignment of the MAGs as well as the phylogenomic reconstruction were performed using GTDB-TK (v0.3.3, release R89) (Chaumeil et al., 2019), classifying 99.6 % of the MAGs as new species, 43.1 % as new genera and 0.1 % as new families. We retained 290 unique genomes, 50 belonging to the Archaea domain and 240 to the Bacteria domain. Two MAGs assembled from Pacbio were not recovered in the Illumina binning. We recovered 75 high-quality genomes (>95 % estimated completeness) across 13 of the 27 archaeal and bacterial phyla detected.

Genome relative abundances across samples were calculated as reads per kilobase of genome per gigabase of metagenome (RPKGs). Raw reads were mapped against MAGs using BLASTn with the following cutoffs: minimum alignment length of 50 bp, minimum identity of 95 %, maximum e-value of 1×10^{-5}. We also estimated the binning efficiency of our datasets. This was determined by mapping raw reads from the metagenomes against all the dereplicated MAGs with Bowtie2. Next, the sum of the mapped reads divided by the total number of reads (i.e. a subsampling of 10 million reads) was used to obtain the average MAG representation.

To establish a robust annotation of the predicted proteins involved in the OM recycling, Carbohydrate-Active enZYmes annotation was performed using run_dbcan (v2.0.11) (Zhang et al., 2018), screened using HMMER (Eddy, 1998), DIAMOND (Buchfink et al., 2015) and Hotpep (Busk et al., 2017) against dbcan, CAZy and PPR databases respectively. Only identical predictions by at least two tools were retained. CAZyme families (or sub-families) have been grouped according to their main characterized enzymatic activities targeting plant biomass (cellulose, hemicellulose), fungal biomass (chitin, glucans), bacterial biomass (peptidoglycan) and phenolic compounds following CAZy database and López-Mondéjar et al. (2020). MAGs metabolic pathways annotation was performed using DRAM (v1.0.0) (Shaffer et al., 2020). Genes were first annotated using Pfam, KOfam, UniProt and MEROPS databases, then classified into functional categories.

2.8. Abundance-weighted Co-occurrence network analysis

A correlation-based network analysis was performed to evaluate abundance-weighted co-occurrences between the 290 MAGs. Co-occurrences were quantified using Spearman's rank correlations calculated between all pairs of MAGs using the RPKG values across the 24 samples, and corrected using the Benjamini-Hochberg standard false discovery rate correction. Only co-occurrences corresponding to correlations with a coefficient (rho) > 0.6 and a p <0.001 were considered to build the network. Modules (i.e., clusters) were computed using the R package *igraph* (Pons and Latapy, 2005), which identifies densely connected communities via random walks. The network visualization was performed using Gephi software (Bastian et al., 2009) with the nodes representing the MAGs and the edges representing the correlations (rho >0.6 and p <0.001) between MAGs.

A random forest analysis was used to test the correct assignment of MAGs to their actual module based on their environmental preferences (i.e., expressed as their individual weighting mean calculated for each environment variable using RPKG data as relative abundance). This analysis was performed using a set of 10,000 trees and the importance of individual variables (i.e., weighting means) in predicting the module assignment was calculated. Models were fitted using the R package *randomForest* (Liaw and Wiener, 2002).

2.9. Virus identification, host prediction and putative AMG annotation

Viral sequences were identified and annotated (AMG) by analyzing all assembled contigs through VIBRANT (v1.0.1) (Kieft et al., 2020) with default parameters (minimum sequence length = 1000bp, minimum open reading frame requirement = 4). Quality (i.e., completeness and contamination) of viral sequences was estimated with CheckV (v0.6) (Nayfach et al., 2021), revealing 55 complete and high-quality genomes (completeness ≥ 90 %). Viral sequences were clustered into 11,524 viral populations based on ANI (≥ 95 %) and shared genes (≥ 80 %). Computational viral host prediction was performed as previously described (Coutinho et al., 2019, 2020; Malki et al., 2021). The Bernadouze bacterial and archaeal MAGs were used as a set of potential host genomes against which the viral genomes were queried. Before performing this analysis, BLAST was used to identify and remove any viral sequences incorrectly binned together with the archaeal and bacterial MAGs. Three signals of virus-host association were analyzed for host prediction: shared tRNAs, homology matches, and CRISPR spacers. Viral sequences were scanned for tRNA genes through tRNAScan-SE (v1.23) (Lowe and Chan, 2016) using the bacterial models. Viral tRNAs were then queried against the Bernadouze MAGs through BLASTn. These searches were performed with the following cutoffs: minimum alignment length of 60 bp, minimum identity of 100 %, minimum query coverage of 95 %, maximum of 0 mismatches and maximum e-value of 1×10^{-3}. Homology matches were performed by directly querying viral sequences against the Bernadouze MAGs through BLASTn. For these searches, the following cutoffs were used: minimum alignment length of 1000 bp, minimum identity of 85 % and maximum e-value of 1×10^{-3}. Finally, CRISPR spacers were identified among Bernadouze MAGs using CRISPRDetect (v2.2) (Biswas et al., 2016). The obtained spacers were queried against the viral sequences using BLASTn. The following cutoffs were defined for these searches: minimum identity of 100 %, minimum query coverage of 100 %, maximum of 0 mismatches and maximum e-value of 1. For each virus-taxon association signal detected (i.e. homology, tRNA or CRISPR), 3 points were added to the taxon if it was a CRISPR match, 2 points if it was a homology match, and 1 point if it was a shared tRNA. The taxon that displayed the highest score was defined as the host of the viral genome. Virus relative abundances in samples were calculated using the same approach used to calculate MAG relative abundance.

2.10. Statistical analyses

All the following statistical analyses were implemented within the R programming environment (RStudio Team, 2020).

The map representing the location of Bernadouze was produced using the R package *sf* (Pebesma, 2018). The influence of the season on the WT depth was analyzed using a Wilcoxon signed-rank test. The difference of C content, N, C:N ratio, DOC, polyphenols (total and soluble), nutrients (SO_4^{2-}, NO_3^-, NH_4^+ and PO_4^{3-}), C accumulation (C content and C density) and soil-atmosphere C exchanges (GPP, ER, NEE) between bog and fen was tested using Wilcoxon signed-rank test. The effect of the environmental parameters on the enzyme activities was tested using an analysis of variance (ANOVA) and compared between bog and fen with a Wilcoxon signed-rank test. The link between these activities on C content was evaluated using Spearman correlations.

The difference of the 16S and 18S gene copy numbers between bog and fen was evaluated using a Wilcoxon signed-rank test. The Bray-Curtis distance was then calculated between all pairs of samples based on 16S rRNA and viral population to study the structure of the microbial

communities, and the results were visualized using non-metric multidimensional scaling ordinations (NMDS) using the function metaMDS in the package *vegan* (Oksanen, 2020). To identify the influence of the environmental variables on the community structure, a dissimilarity matrix was calculated based on Euclidean distances from the 16S rRNA gene or viral population relative abundance estimated in each sample. A first permutational multivariate analysis of variance tests (PerMANOVA) with 9999 iterations (Anderson, 2001) was performed to test the influence of the experimental design namely season, sites, microforms (hummocks and hollows) and depth, including all double interactions using the function adonis2 in *vegan*. A second PerMANOVA was performed to evaluate the influence of environmental parameters (pH, distance to WT, DOC, org C, total N, total phenols, and nutrients). To avoid the presence of strong multicollinearity between the environmental variables, soluble phenols were removed from this analysis since they were strongly correlated with total phenols (Spearman's rank correlation, $r = 0.83$, $p > 0.01$) and a principal component analysis (PCA) was performed between the highly correlated nutrient variables (SO_4^{2-}, NO_3^-, NH_4^+ and PO_4^{3-}). Prior to the PCA, the nutrient variables were scaled to zero mean and unit variance in order to have the same weight in the analysis. Only the first principal component (accounting for 64 %) was kept as a new composite nutrient variable. The metagenome archaeal and bacterial diversity were estimated using the 16S rRNA gene recovered in each metagenome at the species level. The exponential of Shannon ($e^{H'}$) was calculated as alpha diversity metric (Haegeman et al., 2013) using the package *vegan*. These indices were compared between metagenomes using a Wilcoxon signed-rank test.

Finally, an indicator analysis (Dufrêne and Legendre, 1997) was conducted to identify whether the genes involved in OM degradation (plant, fungal and bacterial biomass), polyphenol degradation, fermentation processes (alcohol production, butyrate, propionate, acetate and lactate), methanogenesis and methanotrophy were preferentially associated to either the bog or the fen. This association was assessed using the indicator value (Point-biserial correlation) method (Cáceres and Legendre, 2009) using the package *indicspecies*. This method combines information on the ecological specificity and fidelity of each gene calculated with its respective RPKG distribution across the 24 samples. A permutation test (N = 9999) was used to determine whether a particular gene was significantly associated to either the bog or fen under the null hypothesis of no association.

3. Results

3.1. Geochemical context of the Bernadouze Peatland

The average WT depth in the bog was −10.5 cm and −13.1 cm in the fen, indicating prevalent anoxic conditions (see methods). The pH ranged from 6.4 in the fen to 4.6 in the bog. This is consistent with a shift in vegetation cover: while forbs, sedges and other bushes dominate in the fen, *Sphagnum* mosses are predominant in the bog (Fig. 1A). These variations are congruent with higher concentrations of soluble polyphenols (Wilcoxon, $p < 0.045$, Table S2), and total polyphenols ($p < 0.01$) in the bog than in the fen, while nutrients and N concentrations ($p = 0.569$, $p = 0.976$ respectively) were not significantly different between bog and fen. The C:N ratio did not differ between the bog and the fen ($p = 0.093$, Table S2), suggesting an overall similar peat decomposition.

3.2. Carbon fluxes in bog and fen

We compared the C dynamics in each peatland type by quantifying DOC, C concentration (mass of C per gram of peat) and C density (C concentration multiplied by peat bulk density) which, taken together, evidenced C accumulation. Two-sample Wilcoxon tests (Table S3) revealed a higher DOC concentration ($p = 0.027$) in the bog and C content ($p < 0.01$) whereas we did not observe a difference in C density ($p = 0.881$, Fig. 1A). Overall, the contrast in carbon properties between bog and fen suggests different biotic (decomposition) and/or abiotic (DOC hydrology and geochemistry) processes, which could affect the C dynamics in the two types of peatland. In addition, C properties varied along the peat profile with higher C density at depth in the bog (Fig. S1), consistent with higher C accumulations over time.

Soil-atmosphere C exchanges in the peatland were estimated by measuring field instantaneous C fluxes over six years (2016–2022). The difference between GPP (photosynthetic CO_2 uptake) and ER (autotrophic and heterotrophic CO_2 production), provides an estimation of an ecosystem's C gain and loss, summarized by the NEE. Instantaneous measurements of GPP were always higher than ER at Bernadouze, resulting in a negative NEE (Fig. 1B). However, neither GPP (Wilcoxon, $p = 0.675$), ER ($p = 0.401$) nor NEE ($p = 0.063$, Table S2) showed significant variations between bog and fen, indicating a similar CO_2 fixation and respiration of the two types of peatland. C exchanges were governed by seasonal dynamics, with GPP and ER increasing during the summer season compared to spring, evidencing the importance of temperature and solar radiation on aboveground C dynamics. Together with peat C estimates, these results suggest that the difference in C content between bog and fen at Bernadouze is not due to varying vegetation-related C dynamics. Instead, our findings suggest that differences in belowground C dynamics between bog and fen are sustained by a difference in the magnitude of microbial decomposition.

3.3. Microbial extracellular enzyme activities

We estimated heterotrophic activities related to OM degradation by quantifying the depolymerization of phenolic and lignin-like compounds (phenol oxidase and peroxidase respectively), the degradation of cellulose (β-1,4-glucosidase), the mineralization of organic phosphorus (acid phosphatase), and the hydrolysis of chitin-derived oligomers (β-1,4-N-acetyl-glucosaminidase). Enzyme assays revealed marginal variations between bog and fen (Wilcoxon, $p > 0.05$, Fig. 1C–Table S2), suggesting identical OM degradation. Regression analyses revealed a positive effect of nitrogen concentration on phenol oxidase ($p < 0.001$), peroxidase ($p < 0.001$) and β-glucosidase ($p = 0.01$), a positive effect of the distance to WT on chitinase ($p = 0.047$) and phosphatase ($p = 0.003$), and a positive effect of nutrient concentration on chitinase ($p = 0.007$) (Table S4). In contrast, we noted a negative effect of the distance to the WT on phenol oxidase ($p < 0.001$), indicating a possible phenol degradation under anaerobic conditions. Importantly, free phenolic compound and C content concentrations failed to predict microbial enzyme activities, suggesting (i) that polyphenols do not impede OM degradation and (ii) that C is not a limiting factor for OM degradation. Collectively, these results predict complex relationships between microorganisms and C dynamics.

3.4. Structure and functioning of Peatland microbial communities

We first estimated the prokaryote and fungal abundances based on 16S and 18S gene abundances using qPCR, respectively. No significant difference in prokaryotes (Two-sample Wilcoxon test, $p = 0.320$) or fungal abundances – largely underrepresented – ($p = 0.834$, Table S2) was evidenced between bog and fen. Hypostatizing that a high microbial diversity promotes C degradation and CO_2 emission, we thus compared the prokaryotic diversity based on 16S (exponential of Shannon, $e^{H'}$) with C content. A strong negative correlation (Fig. S2) suggests that higher microbial diversity promotes OM degradation at Bernadouze.

Differences in microbial composition were not significant between spring and summer (PerMANOVA: $R^2 = 0.01$, $p = 0.968$) and between hummock and hollow ($R^2 = 0.03$, $p = 0.352$) (Fig. 2A, Table S5). In contrast, we detected a strong turnover between bog and fen ($R^2 = 0.29$, $p = 0.001$) and with depth ($R^2 = 0.17$, $p = 0.003$), in relation to pH ($R^2 = 0.27$, $p = 0.001$) and distance to the WT ($R^2 = 0.14$, $p = 0.001$). The bog exhibited a lower microbial diversity (Wilcoxon, $p <$ 0.01)

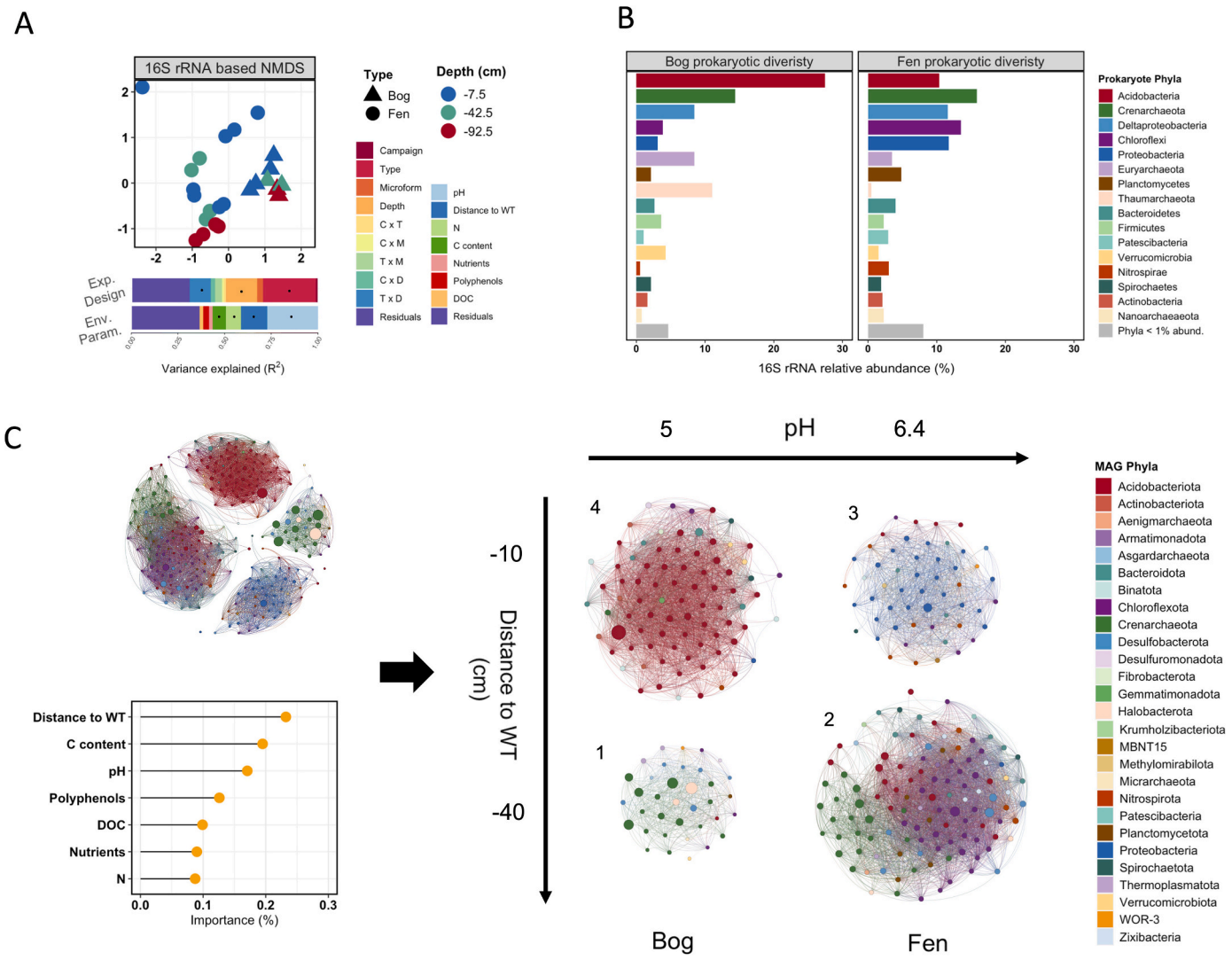

Fig. 2. Environmental drivers of the microbial communities, prokaryotic diversity based on 16S rRNA gene and characterization of the Bernadouze metagenome-assembled genomes (290 dereplicated MAGs). A. Non-metric multidimensional scaling (NMDS) plot of 16S rRNA gene data based on Bray-Curtis distance (stress: 0.10). Below the NMDS, analyses of variance testing the effect of experimental design (Exp. Design): campaign, peatland type, microform, depth, and all possible two-way interactions, and environmental variables (Env. Param.): pH, distance to WT, DOC, C content, N, polyphenols, nutrients, on microbial community structure (16S rRNA based data) using PerMANOVA. Black dots indicate significant correlations (if $p < 0.05$). B. Relative abundance of prokaryotic phyla in the bog and the fen, estimated by unassembled 16S rRNA gene reads. C. Abundance-weighted co-occurrence network based on Spearman correlations calculated from the recruitment values of the 290 unique MAGs with >50 % of completeness and <5 % of contamination (top left). Only significant edges are shown (coefficient >0.6, $p < 0.001$). The size of the nodes is proportional to the cumulative relative abundance of MAGs in the 24 metagenomes. The importance of environmental variables predicting module configuration, estimated by a random forest classification model, is shown in the bottom left. Spatial location of MAGs was estimated using individual weighted means calculated for each environmental variable (pH and distance to WT) using RPKG data as relative abundance (right).

compared to the fen, highlighting environmental filtering due to the acidic conditions in the bog. Acidobacteria (27.5 % of 16S sequences), Crenarchaeota (14.4 %), Thaumarchaeota (11.0 %) and Euryarchaeota (8.4 %) were identified as the dominant phyla in the bog while (Fig. 2B) Crenarchaeota (15.8 %), Chloroflexi (13.5 %), Proteobacteria (11.8 %), Deltaproteobacteria (11.6 %) and Acidobacteria (10.4 %) were the most abundant phyla in the fen.

To identify key microorganisms involved in OM degradation, we reconstructed 290 unique bacterial and archaeal metagenome assembled genomes (MAGs, Fig. 2C). MAG diversity showed a strong congruence with 16S rRNA diversity, with an average number of raw-reads mapping with MAG of 32.5 % in bog and 21.2 % in fen. The ecological niches occupied by these MAGs were estimated through an abundance-weighted co-occurrence network which distinguished four distinct modules (Fig. 2C). Using a random forest classification model, we identified the distance to the WT (0.23 %), C content (0.19 %) and the pH (0.17 %) as the main environmental variables predicting module configuration (Fig. 2C). The similar contribution of pH and C content to module configuration was due to the higher amount of C at acidic pH (Table S2). Modules 1 (36 MAGs) and 4 (81 MAGs) were comprised of MAGs abundant at low pH (pH 5 on average, corresponding to bog conditions) and assigned to deep peat layers for module 1 (−40 cm below the WT) and to the subsurface (−10 cm below the WT) for module 4 (Fig. 2C). The prevalent MAGs (42.7 RPKG on average) were mainly affiliated to the Acidobacteriota and Crenarchaeota phyla. Modules 2 (116 MAGs) and 3 (55 MAGs) were composed of MAGs abundant at circumneutral pH (pH 6.4 on average, corresponding to fen conditions) and were also assigned to deep peat layers for module 2 and to the subsurface for module 3 (Fig. 2C). These MAGs were less abundant on average (26.7 RPKG) but more diverse, mainly belonging to the Crenarchaeota, Chloroflexota, Acidobacteriota, Proteobacteria and Desulfobacterota (Deltaproteobacteria) phyla. Combined with the 16S rRNA

based diversity, these results confirm that the structure of microbial communities in the Bernadouze peatland was driven by pH and depth.

3.5. Role of microorganisms in OM degradation

We examined the CAZYme genes involved in the degradation of OM compounds derived from plants, bacteria and fungi, as well as genes involved in fermentative, methanogenic and methanotrophic pathways (Fig. 3, Table S6). Overall, a large number of MAG-encoded genes involved in the first steps of OM degradation were recovered, highlighting the importance of these processes in peatland C cycling. Particularly, the high abundance of genes involved in the breakdown of cellulose and hemicellulose -which require multiple enzymes-indicated high plant degradation capability. Importantly, 38.3 % of MAG-encoded genes are involved in phenol degradation, supporting the results of enzyme activity assay, and suggesting that phenols can be commonly used as an energy source under anaerobic conditions. In addition, we also found that some abundant groups in the fen such as Gammaproteobacteria, BSN033 (Desulfobacterota) or UBA9217 (Nitrospirota), encoded more genes involved in the recycling of bacterial biomass derived OM than plant-derived OM, which may represent a strategic energy resource under limited OM supply.

An indicator analysis testing the association between pathways and peatland types did not reveal any specific association between pathways and peatland types, indicating that most pathways were found both in fen and bog in similar abundance (Table S7). However, taxa

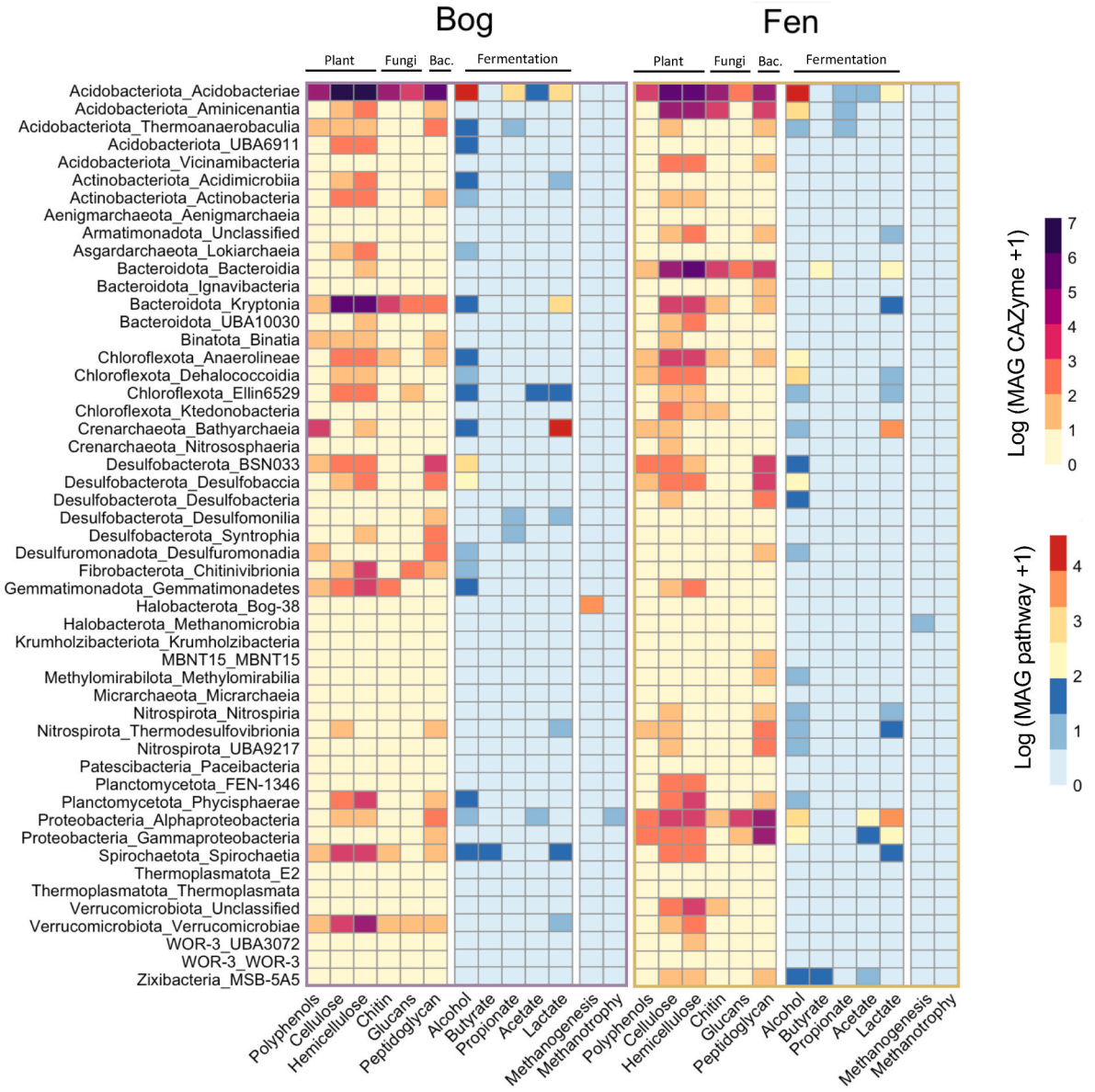

Fig. 3. Predicted metabolic capacities of the Bernadouze MAGs. Heatmap showing the abundance (log (abundance +1)) of MAGs-encoded CAZyme involved in plant biomass degradation (cellulose: GH1, GH3, GH116, GH5, GH6, GH9, GH12, GH45, GH8, AA9, AA10, GH7, GH48, hemicellulose: GH36, GH51, GH54, GH62, GH95, CE1, CE2, CE3, CE4, CE5, CE6, CE7, CE12, CE15, CE16, GH2, GH52, GH120, GH39, GH43, GH26, GH10, GH11, GH30, GH131, GH67, GH115, GH74, GH16, GH44, AA6), fungal biomass degradation (chitin: GH18, GH19, AA11, GH20 and glucans: GH17, GH64, GH81, GH128, GH55), bacterial biomass degradation (peptidoglycan: GH22, GH24, GH25, GH108, GH23, GH73, GH102, GH103, GH104) and polyphenol compounds degradation (K05909, AA1, AA2, K00422) in yellow to purple. The abundances of fermentative (alcohol: K00001, K00121, K04072, K13951, K13952, K13953, K13954, K13980, K18857, butyrate: K00634, K00929, K01896, propionate: K19697, K01026, acetate: K00625, K00925, K01905, K01067, lactate: K00016, K00101, K03778, K03777), methanogenic (K00399, K00401, K00402) and methanotrophic (K10944, K10945, K10946) pathways recovered in MAGs are in light blue to red. The metabolic capacities of MAGs in bog are shown in the left panels (purple frame) and in the right panels (yellow frame) for the fen. These capacities are summed at class-level and log transformed +1.

contribution to each pathway (expressed here as % of RPKG) greatly varied between bog and fen (Fig. 3, Table S8). Importantly, primary functions involved in plant, fungal and bacterial biomass degradation were mostly harbored by the class of Acidobacteriae in the bog (plant OM degradation: 63 %, fungal: 64 % and bacterial: 65 %), surpassing the degradation capacity of Kryptonia (plant: 11 %, fungal: 14 % and bacterial: 11 %) and other taxa. In contrast, taxa contribution to each pathway was more evenly distributed in the fen (Table S8). Acidobacterota appeared as a keystone taxa associated with OM degradation in the Bernadouze peatland and more particularly in the bog.

Subsequent degradation can occur by multiple fermentation processes, including lactate and acetate, but the presence of Acidobacteriae significantly increases the capacity to produce propionate and alcohol in the bog, since they encoded 64 % and 54 % of this fermentative capacity respectively. Ethanol is an important precursor of hydrogenotrophic methanogenesis in the acid bog, and can provide a substrate for the methanogen Bog-38, the most abundant genome assembled at Bernadouze (cumulative relative abundance of Bog-38 = 338 RPKG, means of 290 MAGs = 33 RPKG, Table S9 and Fig. S3) and predominantly recovered in the bog. Similarly to other MAG methanogens, Bog-38 is hydrogenotrophic methanogen (Table S10). Interestingly, CH_4 emissions were lower in the bog than in the fen ($p < 0.01$, Table S2), likely related to the presence of Binataceae (Binatota) and Methylocapsa (Pseudomonadota) methanotrophs that might participate in CO_2 recycling. Overall, these results reveal a similar capacity for OM degradation in the bog and in the fen, consistent with the similar microbial degradation activity and microbial abundances recorded in the two peatland types. Taken together, these results are intriguing given the marked differences in C dynamics (C content and DOC) evidenced between the bog and fen, suggesting that additional regulating processes may drive the differences in C accumulation observed between bog and fen.

3.6. Ecological role of viruses

We identified 14,578 virus sequences in Bernadouze, which clustered into 11,524 viral populations. As with prokaryotic diversity (Fig. 2A), viral diversity was mainly structured according to the pH (PerMANOVA, $R^2 = 0.29$, $p = 0.001$) and the distance to WT ($R^2 = 0.21$, $p = 0.002$), and was stable over time ($p = 0.594$, Fig. 4A). Importantly, viruses were 2.6 times more abundant in the bog than in the fen on average (Fig. 4B), and viral populations for which a host was predicted (24.3 %) were consistently 3 time more in the bog than in the fen

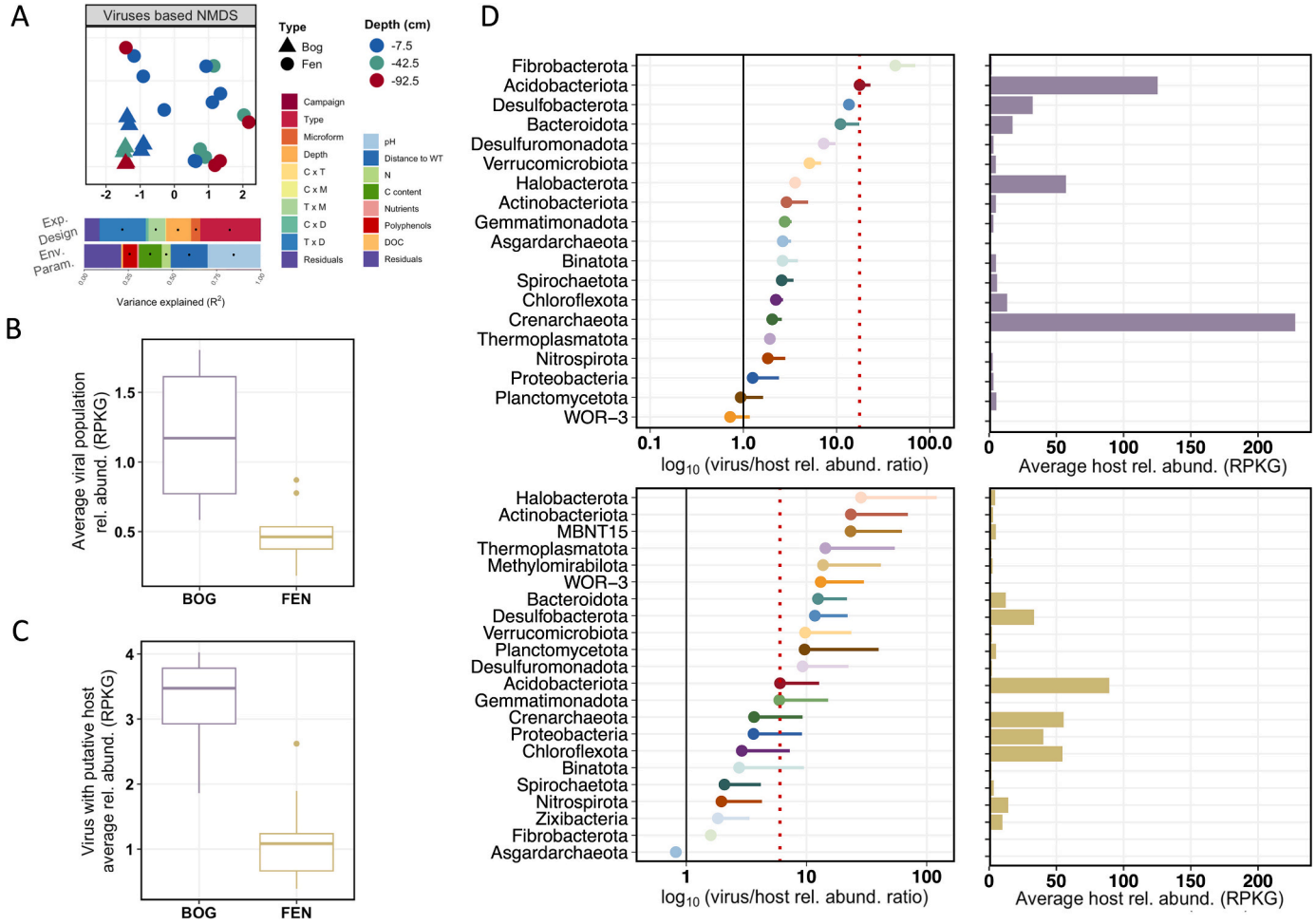

Fig. 4. Environmental drivers and distribution of the viral populations at Bernadouze, predicted prokaryotic host and host-virus relationships in bog and fen A. NMDS plot of the viral populations using Bray-Curtis distance (stress: 0.08). Below the NMDS, analyses of variance testing the effect of experimental design (Exp. Design): campaign, peatland type, microform, depth and all possible two-way interactions, and environmental variables (Env. Param.): pH, distance to WT, DOC, C content, N, polyphenols, nutrients, on viral composition using PerMANOVA. Black dots indicate significant correlation (if $p < 0.05$). B. Average viral population relative abundance in bog and fen samples (expressed in RPKG). C. Box plot representing the average relative abundance of the virus for which a putative host was identified (expressed in RPKG). D. Virus/host relative abundance ratios by host lineage. Relative abundances were calculated from read mapping to viral population and host genomes (both expressed in RPKG), respectively, in bog (top left panel) and in fen (bottom left panel). The dots indicate the mean ratio across samples (in bog n = 8, in fen n = 16), and the error bars indicate one standard deviation. The red line indicates the virus/host relative abundance ratio for the Acidobacteria phylum. The averages host relative abundance in bog and fen are reported on the right panels.

(Fig. 4C). Across the 24 peat samples, virus relative abundance was strongly correlated with host relative abundance at the phylum level, except for poorly represented phyla (Fig. S4). Nevertheless, the bog and the fen exhibited contrasting patterns in terms of viral infection dynamics. In both peatland types, the virus-to-host relative abundance ratio was positive for most phyla, underscoring an overall high level of infection potential at Bernadouze (mean ratio: 6.6 and 9.2 in the bog and the fen respectively). However, this ratio varied greatly between phyla, ranging from 0.72 (WOR-3) to 42.66 (Fibrobacterota) in the bog, and from 0.81 (Asgardarchaeota) to 28.38 (Halobacterota) in the fen. High potential viral infections were recorded for both rare and dominant phyla (Fig. 4D). However, in the case of some phyla, viral infections differed widely between the bog and the fen. Notably, Acidobacteriota – which had the highest potential for OM degradation and was among the most dominant lineages in both peatland types – showed a higher level of infection in the bog (mean virus-to-host relative abundance ratio of 17.65 in the bog and 6.02 in the fen).

Putative AMGs involved in OM degradation were retrieved in 11.4 % of the viral sequences annotated. The most common one, galE, which encodes UDP-glucose 4-epimerase, was recovered 33 times (Table S11). This gene is involved in miscellaneous pathways, as it catalyzes the interconversion of UDP-galactose and UDP-glucose as part of the catabolism of galactose. Although rarely recovered at Bernadouze, putative AMGs involved in the degradation of organic cell compounds (exo-α-sialidase), pectin (pectate lyase) and aromatic compounds (mhpC, carboxymethylenebutenolidase) were also identified, as well as family 18 (chitinase) and family 20 (hexosaminidase) glycosyl hydrolases. Viruses encoding putative AMGs involved in OM degradation were significantly more abundant in the bog than in the fen ($p < 0.001$, Table S11). Overall, we concluded that viruses were more likely to influence the functioning of the bog than the fen.

4. Discussion

We employed a multi-level approach to explain the role of microbial communities in C dynamics in bog and fen, two peatland types recognized to exhibit different C accumulation rates. Carbon accumulation is a long-term process that can take thousands of years (Yu et al., 2010, 2011). We thus investigated contemporary C dynamics through C content, DOC concentration and C density. Contemporary flux exchanges were similar between bog and fen over 6 years of record. Considering that *Sphagnum* mosses produce less biomass than vascular plants (Hobbie and Chapin, 1998), it is unlikely that the higher C content in the bog would be related to a higher OM production. These results were supported by the heterotrophic activity involved in OM degradation, also found to be similar between bog and fen. Considering that these activities are correlated with nutrient concentrations, a nutrient limitation may contribute to the C accumulation process at the peatland scale (Dorrepaal et al., 2005; Turetsky, 2003). However, nutrients cannot be considered the source of differences in C content at Bernadouze given that their concentration was similar in the bog and in the fen. Also, contrary to the "enzyme latch theory" (Fenner and Freeman, 2011; Freeman et al., 2001), which suggests that phenolic compounds can act as a "latch" to stabilize C in the peat, we did not identify any significant relationship linking polyphenols (total and soluble) and microbial extracellular enzymatic activities. Moreover, 38.3 % of MAGs possessed the metabolic capacity to use phenolic compounds as an energy source, which thus may represent a sustainable source of OM for microorganisms, mainly under anaerobic conditions, as recently demonstrated (McGivern et al., 2021).

The present work confirmed that Acidobacteriota, the predominant lineage in the Bernadouze peatland, exhibited a high metabolic capacity for OM degradation. They encoded the largest repertoire of CAZymes in the peatland, a consistent feature observed in cultivable Acidobacteria (Eichorst et al., 2007; Pankratov and Dedysh, 2010; Whang et al., 2014), as well as in genomes assembled from natural environments (Diamond et al., 2019; Woodcroft et al., 2018). Acidobacteriota dominated the microbial community in the bog where environmental conditions fit their ecological niches (Kalam et al., 2020). Their high metabolic capacity in OM degradation contrasted therefore with the C dynamics in the bog, where higher C content and DOC concentration were recorded. Interestingly, we also established that the bog contained 2.6 times more viruses than the fen and that bog Acidobacteriota were probably subject to higher pressure of viral infection than their fen counterparts.

The higher relative abundance of viruses in the bog, consistent with Emerson et al. (2018) findings, might be due to higher viral adsorption to soil surfaces at acidic pH (Gerba, 1984). However, not all host taxa in the Bernadouze bog exhibit higher virus/host ratio. While a higher number of virus predicted to infect Acidobacteriota were also found in the thawing permafrost of Stordalen (Emerson et al., 2018), the Acidobacteriota virus/host ratio was higher in the Bernadouze bog (17.65) compared to thawing permafrost (0.1–1). These results are in line to the *Kill the Winner* model, in which viruses exert a top-down control over microbial community by targeting the most abundant taxa (Thingstad, 2000). The high abundance of virus predicted to infect Acidobacteriota might contribute to constrain their metabolic rate (Feiner et al., 2015; Paul, 2008) and impair their efficiency in degrading OM in the bog. Moreover, although we cannot evidence a difference in the viral infection dynamics across the two seasons, viral shunts, that result in host-selective viral lysis and death, further exacerbates their role in bog C dynamics by altering C degradation capacity. Interestingly, the release of carbon and nutrients into the milieu as a consequence of cells bursting might contribute to explain the higher DOC concentration we evidenced in the Bernadouze bog, a process previously suggested in the Stordalen frozen peatland (Emerson et al., 2018). Consequently, we propose that the role of bog viruses may be underestimated, as they impair OM degradation by primary degraders, thereby enhancing C accumulation over time. However, we are aware that additional factors such as slow growth (Campanharo et al., 2016; Davis et al., 2005, 2011; George et al., 2011) and slower degradation rates (Pankratov et al., 2011) in Acidobacteria might also contribute to impair OM degradation in the bog.

We have also evidenced negative associations between microbial diversity and C content at Bernadouze. Consistent with previous studies (Finn et al., 2020; Seward et al., 2020; St. James et al., 2021), the bog has been characterized as having a low microbial diversity, dominated by a few lineages belonging to Acidobacteria, whereas the fen exhibits more diverse microbial communities, mainly composed of Proteobacteria, Crenarchaeota, Acidobacteria, Deltaproteobacteria and Chloroflexi. It has been demonstrated that a high microbial diversity promotes organic matter decomposition in soils (Maron et al., 2018). Therefore, the lower bog microbial diversity could also be a factor in reduced OM decomposition. High microbial diversity might improve cross-feeding (van Hoek and Merks, 2017), minimizing enzyme and intermediate concentrations in a pathway, maximizing ATP production within the community, and stimulating OM degradation (Pfeiffer and Bonhoeffer, 2004; Wei et al., 2009). The acidic pH prevailing in the bog would instead result in a specialization and metabolic capacity overlap (Hester et al., 2019), preventing efficient OM degradation.

Overall, these results provide evidence that bog and fen are two distinct ecosystems that not only differ by their environmental conditions but also by the composition of their prokaryotic and viral communities. Consequently, we showed that the functioning of these ecosystems, and particularly their C dynamics, is not only driven by ecological gradients, trophic status, vegetation covers and hydrology but also by unique microbial communities that directly drive OM turnover. Hence, we highlighted that a higher C content and DOC concentration in the bog, reflecting a lower OM degradation capacity, might be the result of i) a disruption in the metabolic potential of Acidobacteriota key degraders due to their susceptibility to viral predation and ii) the high specialization and metabolic overlap within the bog microbial community. Understanding the extent to which each of these processes contributes to disrupting OM degradation in bog and fen is of paramount

importance to quantify the ecological and biogeochemical outcomes of peatland functions and assess their impact on C accumulation over time in the context of climate change.

CRediT authorship contribution statement

Etienne Richy: Writing – original draft, Visualization, Methodology, Investigation, Formal analysis, Data curation, Conceptualization. **Pedro J. Cabello-Yeves:** Writing – review & editing, Supervision, Methodology. **Felipe Hernandes-Coutinho:** Writing – review & editing, Supervision, Methodology. **Francisco Rodriguez-Valera:** Writing – review & editing, Supervision. **Iván González-Álvarez:** Methodology, Formal analysis. **Laure Gandois:** Writing – review & editing, Validation, Methodology, Formal analysis. **François Rigal:** Writing – review & editing, Visualization, Validation, Supervision, Methodology, Investigation, Formal analysis, Data curation, Conceptualization. **Béatrice Lauga:** Writing – review & editing, Validation, Supervision, Project administration, Methodology, Investigation, Funding acquisition, Formal analysis, Data curation, Conceptualization.

Declaration of competing interest

The authors declare that they have no known competing financial interests or personal relationships that could have appeared to influence the work reported in this paper.

Data availability

Genomic data, including raw Illumina sequencing reads of the 24 metagenomes (SAMN24979748- SAMN24979725), the 2 raw Pacbio sequencing reads (SAMN26257891, SAMN26256348), the 290 MAGs (SAMN25001521-SAMN25001810), and the 11,755 viral populations (SAMN26259414) are available under NCBI BioProject accession number PRJNA797241.

Acknowledgments

The authors thank F. Julien, V. Payre-Suc and D. Lambrigot for DOC and major elements analysis (PAPC platform, EcoLab laboratory); and Simon Gascoin, Pascal Fanise, the CESBIO laboratory and the OSR Toulouse for providing the meteorological data. We are indebted to Alice Baldy and Eva Sandoval-Quintana for their fieldwork support, Vincent E. J. Jassey for his advice regarding enzyme activity assays, and Dominique Masse for the English revision of the manuscript. This project was co-funded by the LabEx DRIIHM OHM Haut Vicdessos/Haute Vallée des Gaves (DRIIHM/IRDHEI - ANR-11-LABX-0010 LABX – 2011, Pyrpeat project), INTERREG V POCTEFA REPLIM (project no. EFA056/15). B.L. was supported by funds from E2S-UPPA (E2S - ANR-16-IDEX-0002 - Hub-MeSMic). E.R. was supported by a PhD grant from the CDABPP (Communauté d'Agglomération Pau Béarn Pyrénées) and IPREM, and by a postdoctoral fellowship from E2S-UPPA (E2S - ANR-16-IDEX-0002). I. G.A. was supported by an Académie des talents graduate fellowship from E2S-UPPA (E2S - ANR-16-IDEX-0002). PJC-Y was supported by an APOSTD/2019/009 Postdoctoral fellowship from Generalitat Valenciana.

Appendix A. Supplementary data

Supplementary data to this article can be found online at https://doi.org/10.1016/j.soilbio.2024.109345.

References

Abdalla, M., Hastings, A., Truu, J., Espenberg, M., Mander, Ü., Smith, P., 2016. Emissions of methane from northern peatlands: a review of management impacts and implications for future management options. Ecology and Evolution 6, 7080–7102. https://doi.org/10.1002/ece3.2469.

Altschul, S.F., Gish, W., Miller, W., Myers, E.W., Lipman, D.J., 1990. Basic local alignment search tool. Journal of Molecular Biology 3, 403–410.

Anderson, M.J., 2001. A new method for non-parametric multivariate analysis of variance. Austral Ecology 26, 32–46. https://doi.org/10.1111/j.1442-9993.2001.01070.

Bastian, M., Heymann, S., Jacomy, M., 2009. Gephi : an Open Source Software for Exploring and Manipulating Networks 2.

Bengtsson, F., Rydin, H., Hájek, T., 2018. Biochemical determinants of litter quality in 15 species of Sphagnum. Plant and Soil 425, 161–176. https://doi.org/10.1007/s11104-018-3579-8.

Biswas, A., Staals, R.H.J., Morales, S.E., Fineran, P.C., Brown, C.M., 2016. CRISPRDetect: a flexible algorithm to define CRISPR arrays. BMC Genomics 17, 356. https://doi.org/10.1186/s12864-016-2627-0.

Bolger, A.M., Lohse, M., Usadel, B., 2014. Trimmomatic: a flexible trimmer for Illumina sequence data. Bioinformatics 30, 2114–2120. https://doi.org/10.1093/bioinformatics/btu170.

Borneman, J., Hartin, R.J., 2000. PCR primers that amplify fungal rRNA genes from environmental samples. Applications in Environmental Microbiology 66, 4356–4360.

Bragazza, L., Siffi, C., Iacumin, P., Gerdol, R., 2007. Mass loss and nutrient release during litter decay in peatland: the role of microbial adaptability to litter chemistry. Soil Biology and Biochemistry 39, 257–267. https://doi.org/10.1016/j.soilbio.2006.07.014.

Buchfink, B., Xie, C., Huson, D.H., 2015. Fast and sensitive protein alignment using DIAMOND. Nature Methods 12, 59–60. https://doi.org/10.1038/nmeth.3176.

Busk, P.K., Pilgaard, B., Lezyk, M.J., Meyer, A.S., Lange, L., 2017. Homology to peptide pattern for annotation of carbohydrate-active enzymes and prediction of function. BMC Bioinformatics 18, 1–9.

Cabello-Yeves, P.J., Zemskaya, T.I., Zakharenko, A.S., Sakirko, M.V., Ivanov, V.G., Ghai, R., Rodriguez-Valera, F., 2020. Microbiome of the deep Lake Baikal, a unique oxic bathypelagic habitat. Limnology & Oceanography 65, 1471–1488. https://doi.org/10.1002/lno.11401.

Cáceres, M.D., Legendre, P., 2009. Associations between species and groups of sites: indices and statistical inference. Ecology 90, 3566–3574. https://doi.org/10.1890/08-1823.1.

Campanharo, J.C., Kielak, A.M., Castellane, T.C.L., Kuramae, E.E., Lemos, E.G. de M., 2016. Optimized medium culture for *Acidobacteria* subdivision 1 strains. FEMS Microbiology Letters 363, fnw245. https://doi.org/10.1093/femsle/fnw245.

Chaumeil, P.-A., Mussig, A.J., Hugenholtz, P., Parks, D.H., 2019. GTDB-Tk: a toolkit to classify genomes with the Genome Taxonomy Database. Bioinformatics btz848. https://doi.org/10.1093/bioinformatics/btz848.

Chen, L.-X., Méheust, R., Crits-Christoph, A., McMahon, K.D., Nelson, T.C., Slater, G.F., Warren, L.A., Banfield, J.F., 2020. Large freshwater phages with the potential to augment aerobic methane oxidation. Nat. Microbiol. 5, 1504–1515. https://doi.org/10.1038/s41564-020-0779-9.

Coutinho, F.H., Cabello-Yeves, P.J., Gonzalez-Serrano, R., Rosselli, R., López-Pérez, M., Zemskaya, T.I., Zakharenko, A.S., Ivanov, V.G., Rodriguez-Valera, F., 2020. New viral biogeochemical roles revealed through metagenomic analysis of Lake Baikal. Microbiome 8, 163. https://doi.org/10.1186/s40168-020-00936-4.

Coutinho, F.H., Rosselli, R., Rodríguez-Valera, F., 2019. Trends of microdiversity reveal depth-dependent evolutionary strategies of viruses in the Mediterranean. mSystems 4, e00554-19. https://doi.org/10.1128/mSystems.00554-19.

Dalcin Martins, P., Danczak, R.E., Roux, S., Frank, J., Borton, M.A., Wolfe, R.A., Burris, M.N., Wilkins, M.J., 2018. Viral and metabolic controls on high rates of microbial sulfur and carbon cycling in wetland ecosystems. Microbiome 6, 138. https://doi.org/10.1186/s40168-018-0522-4.

Danevčič, T., Mandic-Mulec, I., Stres, B., Stopar, D., Hacin, J., 2010. Emissions of CO2, CH4 and N2O from southern European peatlands. Soil Biology and Biochemistry 42, 1437–1446. https://doi.org/10.1016/j.soilbio.2010.05.004.

Davis, K.E.R., Joseph, S.J., Janssen, P.H., 2005. Effects of growth medium, inoculum size, and incubation time on culturability and isolation of soil bacteria. Applied and Environmental Microbiology 71, 826–834. https://doi.org/10.1128/AEM.71.2.826-834.2005.

Davis, K.E.R., Sangwan, P., Janssen, P.H., 2011. Acidobacteria, Rubrobacteridae and Chloroflexi are abundant among very slow-growing and mini-colony-forming soil bacteria: slow-growing and mini-colony-forming soil bacteria. Environmental Microbiology 13, 798–805. https://doi.org/10.1111/j.1462-2920.2010.02384.x.

Diamond, S., Andeer, P.F., Li, Z., Crits-Christoph, A., Burstein, D., Anantharaman, K., Lane, K.R., Thomas, B.C., Pan, C., Northen, T.R., Banfield, J.F., 2019. Mediterranean grassland soil C–N compound turnover is dependent on rainfall and depth, and is mediated by genomically divergent microorganisms. Nat. Microbiol. 4, 16.

Dorrepaal, E., Cornelissen, J.H.C., Aerts, R., Wallén, B., Van Logtestijn, R.S.P., 2005. Are growth forms consistent predictors of leaf litter quality and decomposability across peatlands along a latitudinal gradient? Journal of Ecology 93, 817–828. https://doi.org/10.1111/j.1365-2745.2005.01024.x.

Drake, H.L., Horn, M.A., Wüst, P.K., 2009. Intermediary ecosystem metabolism as a main driver of methanogenesis in acidic wetland soil: drivers of methanogenesis in fen soil. Environ. Microbiol. Rep. 1, 307–318. https://doi.org/10.1111/j.1758-2229.2009.00050.x.

Dufrêne, M., Legendre, P., 1997. Species assemblages and indicator species: the need for a flexible asymmetrical approach. Ecological Monographs 67, 22.

Eddy, S.R., 1998. Profile hidden Markov models. Bioinformatics 14, 755–763. https://doi.org/10.1093/bioinformatics/14.9.755.

Edgar, R.C., 2010. Search and clustering orders of magnitude faster than BLAST. Bioinformatics 26, 2460–2461.

Eichorst, S.A., Breznak, J.A., Schmidt, T.M., 2007. Isolation and characterization of soil bacteria that define Terriglobus gen. nov., in the phylum Acidobacteria. Applied and Environmental Microbiology 73, 10.
Emerson, J.B., Roux, S., Brum, J.R., Bolduc, B., Woodcroft, B.J., Jang, H.B., Singleton, C. M., Solden, L.M., Naas, A.E., Boyd, J.A., Hodgkins, S.B., Wilson, R.M., Trubl, G., Li, C., Frolking, S., Pope, P.B., Wrighton, K.C., Crill, P.M., Chanton, J.P., Saleska, S. R., Tyson, G.W., Rich, V.I., Sullivan, M.B., 2018. Host-linked soil viral ecology along a permafrost thaw gradient. Nat. Microbiol. 3, 870–880. https://doi.org/10.1038/s41564-018-0190-y.
Feiner, R., Argov, T., Rabinovich, L., Sigal, N., Borovok, I., Herskovits, A.A., 2015. A new perspective on lysogeny: prophages as active regulatory switches of bacteria. Nature Reviews Microbiology 13, 641–650. https://doi.org/10.1038/nrmicro3527.
Fenner, N., Freeman, C., 2011. Drought-induced carbon loss in peatlands. Nature Geoscience 4, 895–900. https://doi.org/10.1038/ngeo1323.
Finn, D.R., Ziv-El, M., van Haren, J., Park, J.G., del Aguila-Pasquel, J., Urquiza–Muñoz, J. D., Cadillo-Quiroz, H., 2020. Methanogens and methanotrophs show nutrient-dependent community assemblage patterns across tropical peatlands of the Pastaza-Marañón basin, Peruvian Amazonia. Frontiers in Microbiology 11, 746. https://doi.org/10.3389/fmicb.2020.00746.
Freeman, C., Ostle, N., Kang, H., 2001. An enzymic "latch" on a global carbon store. Nature 409. https://doi.org/10.1038/35051650, 149–149.
George, I.F., Hartmann, M., Liles, M.R., Agathos, S.N., 2011. Recovery of as-yet-uncultured soil Acidobacteria on dilute solid media. Applied and Environmental Microbiology 77, 8184–8188. https://doi.org/10.1128/AEM.05956-11.
Gerba, C.P., 1984. Applied and theoretical aspects of virus adsorption to surfaces. In: Adv. Appl. Microbiol. Elsevier, pp. 133–168. https://doi.org/10.1016/S0065-2164(08)70054-6.
Haegeman, B., Hamelin, J., Moriarty, J., Neal, P., Dushoff, J., Weitz, J.S., 2013. Robust estimation of microbial diversity in theory and in practice. ISME Journal 7, 1092–1101. https://doi.org/10.1038/ismej.2013.10.
Hester, E.R., Jetten, M.S.M., Welte, C.U., Lücker, S., 2019. Metabolic overlap in environmentally diverse microbial communities. Frontiers in Genetics 10, 989. https://doi.org/10.3389/fgene.2019.00989.
Hobbie, S.E., Chapin, F.S., 1998. The response of tundra plant biomass, aboveground production, nitrogen, and CO2 Flux to experimental warming. Ecology 79, 1526. https://doi.org/10.2307/176774.
van Hoek, M.J.A., Merks, R.M.H., 2017. Emergence of microbial diversity due to cross-feeding interactions in a spatial model of gut microbial metabolism. BMC Systems Biology 11, 56. https://doi.org/10.1186/s12918-017-0430-4.
Horn, M.A., Matthies, C., Küsel, K., Schramm, A., Drake, H.L., 2003. Hydrogenotrophic methanogenesis by moderately acid-tolerant methanogens of a methane-emitting acidic peat. Applied and Environmental Microbiology 69, 74–83. https://doi.org/10.1128/AEM.69.1.74-83.2003.
Hoyos-Santillan, J., Lomax, B.H., Turner, B.L., Sjögersten, S., 2018. Nutrient limitation or home field advantage: does microbial community adaptation overcome nutrient limitation of litter decomposition in a tropical peatland? Journal of Ecology 106, 1558–1569. https://doi.org/10.1111/1365-2745.12923.
Hugelius, G., Loisel, J., Chadburn, S., Jackson, R.B., Jones, M., MacDonald, G., Marushchak, M., Olefeldt, D., Packalen, M., Siewert, M.B., Treat, C., Turetsky, M., Voigt, C., Yu, Z., 2020. Large stocks of peatland carbon and nitrogen are vulnerable to permafrost thaw. Proceedings of the National Academy of Sciences 117, 20438–20446. https://doi.org/10.1073/pnas.1916387117.
Jalut, G., Delibrias, G., Dagnac, J., Mardones, M., 1982. A Palaeoecological Approach to the Last 21 000 Years in the Pyrenees: the Peat Bog of Freychinede (Alt. 1350 M, Ariege, South France), 33.
Jansson, J.K., Taş, N., 2014. The microbial ecology of permafrost. Nature Reviews Microbiology 12, 414–425. https://doi.org/10.1038/nrmicro3262.
Jones, D., Willett, V., 2006. Experimental evaluation of methods to quantify dissolved organic nitrogen (DON) and dissolved organic carbon (DOC) in soil. Soil Biology and Biochemistry 38, 991–999. https://doi.org/10.1016/j.soilbio.2005.08.012.
Joosten, H., Clarke, D., 2002. Wise Use of Mires and Peatlands, vol. 304. International Peat Society and international Mire Conservation Group.
Kalam, S., Basu, A., Ahmad, I., Sayyed, R.Z., El-Enshasy, H.A., Dailin, D.J., Suriani, N.L., 2020. Recent understanding of soil Acidobacteria and their ecological significance: a critical review. Frontiers in Microbiology 11, 580024. https://doi.org/10.3389/fmicb.2020.580024.
Kang, D.D., Li, F., Kirton, E., Thomas, A., Egan, R., An, H., Wang, Z., 2019. MetaBAT 2: an adaptive binning algorithm for robust and efficient genome reconstruction from metagenome assemblies. PeerJ 7, e7359. https://doi.org/10.7717/peerj.7359.
Kieft, K., Zhou, Z., Anantharaman, K., 2020. VIBRANT: automated recovery, annotation and curation of microbial viruses, and evaluation of viral community function from genomic sequences. Microbiome 8, 90. https://doi.org/10.1186/s40168-020-00867-0.
Lang, S.I., Cornelissen, J.H.C., Klahn, T., van Logtestijn, R.S.P., Broekman, R., Schweikert, W., Aerts, R., 2009. An experimental comparison of chemical traits and litter decomposition rates in a diverse range of subarctic bryophyte, lichen and vascular plant species. Journal of Ecology 97, 886–900. https://doi.org/10.1111/j.1365-2745.2009.01538.x.
Langmead, B., Salzberg, S.L., 2012. Fast gapped-read alignment with Bowtie 2. Nature Methods 9, 357–359. https://doi.org/10.1038/nmeth.1923.
Liaw, A., Wiener, M., 2002. Classification and regression by randomForest. R News 2, 5.
Lin, X., Green, S., Tfaily, M.M., Prakash, O., Konstantinidis, K.T., Corbett, J.E., Chanton, J.P., Cooper, W.T., Kostka, J.E., 2012. Microbial community structure and activity linked to contrasting biogeochemical gradients in bog and fen environments of the glacial lake agassiz peatland. Applied and Environmental Microbiology 78, 7023–7031. https://doi.org/10.1128/AEM.01750-12.
Loisel, J., Gallego-Sala, A.V., Amesbury, M.J., Magnan, G., Anshari, G., Beilman, D.W., Benavides, J.C., Blewett, J., Camill, P., Charman, D.J., Chawchai, S., Hedgpeth, A., Kleinen, T., Korhola, A., Large, D., Mansilla, C.A., Müller, J., van Bellen, S., West, J. B., Yu, Z., Bubier, J.L., Garneau, M., Moore, T., Sannel, A.B.K., Page, S., Väliranta, M., Bechtold, M., Brovkin, V., Cole, L.E.S., Chanton, J.P., Christensen, T. R., Davies, M.A., De Vleeschouwer, F., Finkelstein, S.A., Frolking, S., Gałka, M., Gandois, L., Girkin, N., Harris, L.I., Heinemeyer, A., Hoyt, A.M., Jones, M.C., Joos, F., Juutinen, S., Kaiser, K., Lacourse, T., Lamentowicz, M., Larmola, T., Leifeld, J., Lohila, A., Milner, A.M., Minkkinen, K., Moss, P., Naafs, B.D.A., Nichols, J., O'Donnell, J., Payne, R., Philben, M., Piilo, S., Quillet, A., Ratnayake, A. S., Roland, T.P., Sjögersten, S., Sonnentag, O., Swindles, G.T., Swinnen, W., Talbot, J., Treat, C., Valach, A.C., Wu, J., 2021. Expert assessment of future vulnerability of the global peatland carbon sink. Nature Climate Change 11, 70–77. https://doi.org/10.1038/s41558-020-00944-0.
López-Mondéjar, R., Tláskal, V., Větrovský, T., Štursová, M., Toscan, R., Nunes da Rocha, U., Baldrian, P., 2020. Metagenomics and stable isotope probing reveal the complementary contribution of fungal and bacterial communities in the recycling of dead biomass in forest soil. Soil Biology and Biochemistry 148, 107875. https://doi.org/10.1016/j.soilbio.2020.107875.
Lowe, T.M., Chan, P.P., 2016. tRNAscan-SE On-line: integrating search and context for analysis of transfer RNA genes. Nucleic Acids Research 44, W54–W57. https://doi.org/10.1093/nar/gkw413.
Lopez-Gutierrez, J.C., Henry, S., Hallet, S., Martin-Laurent, F., Catroux, G., Philippot, L., 2004. Quantification of a novel group of nitrate-reducing bacteria in the environment by real- time PCR. Journal of Microbiological Methods 57, 399–407.
Malki, K., Sawaya, N.A., Tisza, M.J., Coutinho, F.H., Rosario, K., Székely, A.J., Breitbart, M., 2021. Spatial and temporal dynamics of prokaryotic and viral community assemblages in a lotic system (Manatee Springs, Florida). Applied and Environmental Microbiology 87, e00646-21. https://doi.org/10.1128/AEM.00646-21.
Maron, P.-A., Sarr, A., Kaisermann, A., Lévêque, J., Mathieu, O., Guigue, J., Karimi, B., Bernard, L., Dequiedt, S., Terrat, S., Chabbi, A., Ranjard, L., 2018. High microbial diversity promotes soil ecosystem functioning. Applied and Environmental Microbiology 84, e02738-17. https://doi.org/10.1128/AEM.02738-17.
McGivern, B.B., Tfaily, M.M., Borton, M.A., Kosina, S.M., Daly, R.A., Nicora, C.D., Purvine, S.O., Wong, A.R., Lipton, M.S., Hoyt, D.W., Northen, T.R., Hagerman, A.E., Wrighton, K.C., 2021. Decrypting bacterial polyphenol metabolism in an anoxic wetland soil. Nature Communications 12, 2466. https://doi.org/10.1038/s41467-021-22765-1.
Muyzer, G., de Waal, E.C., Uitterlinden, A.G., 1993. Profiling of complex microbial populations by denaturing gradient gel electrophoresis analysis of polymerase chain reaction- amplified genes coding for 16S rRNA. Applied and Environmental Microbiology 59, 695–700.
Nawrocki, E.P., Eddy, S.R., 2010. Ssu-Align: a Tool for Structural Alignment of SSU rRNA Sequences.
Nayfach, S., Camargo, A.P., Schulz, F., Eloe-Fadrosh, E., Roux, S., Kyrpides, N.C., 2021. CheckV assesses the quality and completeness of metagenome-assembled viral genomes. Nature Biotechnology 39, 578–585. https://doi.org/10.1038/s41587-020-00774-7.
Oksanen, J., 2020. Vegan: ecological diversity 12.
Pankratov, T.A., Dedysh, S.N., 2010. *Granulicella paludicola* gen. nov., sp. nov., *Granulicella pectinivorans* sp. nov., *Granulicella aggregans* sp. nov. and *Granulicella rosea* sp. nov., acidophilic, polymer-degrading acidobacteria from Sphagnum peat bogs. International Journal of Systematic and Evolutionary Microbiology 60, 2951–2959. https://doi.org/10.1099/ijs.0.021824-0.
Pankratov, T.A., Ivanova, A.O., Dedysh, S.N., Liesack, W., 2011. Bacterial populations and environmental factors controlling cellulose degradation in an acidic Sphagnum peat: cellulose degradation in acidic peat. Environmental Microbiology 13, 1800–1814. https://doi.org/10.1111/j.1462-2920.2011.02491.x.
Parks, D.H., Imelfort, M., Skennerton, C.T., Hugenholtz, P., Tyson, G.W., 2015. CheckM: assessing the quality of microbial genomes recovered from isolates, single cells, and metagenomes. Genome Research 25, 1043–1055. https://doi.org/10.1101/gr.186072.114.
Paul, J.H., 2008. Prophages in marine bacteria: dangerous molecular time bombs or the key to survival in the seas? ISME Journal 2, 579–589. https://doi.org/10.1038/ismej.2008.35.
Pebesma, E., 2018. Simple features for R: standardized support for spatial vector data. R J 10, 439. https://doi.org/10.32614/RJ-2018-009.
Peng, Y., Leung, H.C.M., Yiu, S.M., Chin, F.Y.L., 2012. IDBA-UD: a de novo assembler for single-cell and metagenomic sequencing data with highly uneven depth. Bioinformatics 28, 1420–1428. https://doi.org/10.1093/bioinformatics/bts174.
Pfeiffer, T., Bonhoeffer, S., 2004. Evolution of cross-feeding in microbial populations. The American Naturalist 163, E126–E135. https://doi.org/10.1086/383593.
Pons, P., Latapy, M., 2005. Computing Communities in Large Networks Using Random Walks (Long Version) arXiv:physics/0512106.
Preston, M.D., Smemo, K.A., McLaughlin, J.W., Basiliko, N., 2012. Peatland microbial communities and decomposition processes in the James Bay Lowlands, Canada. Frontiers in Microbiology 3, 1–15. https://doi.org/10.3389/fmicb.2012.00070.
Prjibelski, A., Antipov, D., Meleshko, D., Lapidus, A., Korobeynikov, A., 2020. Using SPAdes de novo assembler. Curr. Protoc. Bioinforma. 70 https://doi.org/10.1002/cpbi.102.
Quast, C., Pruesse, E., Yilmaz, P., Gerken, J., Schweer, T., Yarza, P., Peplies, J., Glöckner, F.O., 2012. The SILVA ribosomal RNA gene database project: improved data processing and web-based tools. Nucleic Acids Research 41, D590–D596. https://doi.org/10.1093/nar/gks1219.

Reille, M., 1990. Recherches pollenanalytiques dans l'extrémité orientale des Pyrénées : données nouvelles, de la fin du Glaciaire à l'Actuel. Ecologia Mediterranea 16, 317–357. https://doi.org/10.3406/ecmed.1990.1673.

Rosset, T., Gandois, L., Le Roux, G., Teisserenc, R., Durantez Jimenez, P., Camboulive, T., Binet, S., 2019. Peatland contribution to stream organic carbon exports from a montane watershed. J. Geophys. Res. Biogeosciences 124, 3448–3464. https://doi.org/10.1029/2019JG005142.

RStudio Team, 2020. RStudio: Integrated Development Environment for R. RStudio. PBC, Boston, MA. http://www.rstudio.com/.

Rydin, H., Jeglum, J.K., Hooijer, A., 2006. The Biology of Peatlands, the Biology of Habitats. Oxford University Press, Oxford ; New York.

Seward, J., Carson, M.A., Lamit, L.J., Basiliko, N., Yavitt, J.B., Lilleskov, E., Schadt, C.W., Smith, D.S., Mclaughlin, J., Mykytczuk, N., Willims-Johnson, S., Roulet, N., Moore, T., Harris, L., Bräuer, S., 2020. Peatland microbial community composition is driven by a natural climate gradient. Microbial Ecology 80, 593–602. https://doi.org/10.1007/s00248-020-01510-z.

Shaffer, M., Borton, M.A., McGivern, B.B., Zayed, A.A., La Rosa, S.L., Solden, L.M., Liu, P., Narrowe, A.B., Rodríguez-Ramos, J., Bolduc, B., Gazitúa, M.C., Daly, R.A., Smith, G.J., Vik, D.R., Pope, P.B., Sullivan, M.B., Roux, S., Wrighton, K.C., 2020. DRAM for distilling microbial metabolism to automate the curation of microbiome function. Nucleic Acids Research 48, 8883–8900. https://doi.org/10.1093/nar/gkaa621.

St James, A.R., Lin, J., Richardson, R.E., 2021. Relationship between peat type and microbial ecology in Sphagnum-containing peatlands of the Adirondack mountains. Microbial Ecology. https://doi.org/10.1007/s00248-020-01651-1. NY, USA.

Thingstad, T.F., 2000. Elements of a theory for the mechanisms controlling abundance, diversity, and biogeochemical role of lytic bacterial viruses in aquatic systems. Limnology & Oceanography 45, 1320–1328. https://doi.org/10.4319/lo.2000.45.6.1320.

Thormann, M.N., Szumigalski, A.R., Bayley, S.E., 1999. Aboveground peat and carbon accumulation potentials along a bog-fen-marsh wetland gradient in southern boreal Alberta, Canada. Wetlands 19, 305–317. https://doi.org/10.1007/BF03161761.

Trubl, G., Jang, H. bin, Roux, S., Emerson, J.B., Brum, J.R., Bolduc, B., Woodcroft, B.J., Jang, H.B., Singleton, C.M., Solden, L.M., Naas, A.E., Boyd, J.A., Hodgkins, S.B., Wilson, R.M., Li, C., Frolking, S., Pope, P.B., Wrighton, K.C., Crill, P.M., Chanton, J. P., Saleska, S.R., Tyson, G.W., Rich, V.I., Sullivan, M.B., 2018. Soil viruses are underexplored players in ecosystem carbon processing. Nat. Microbiol. 3, 870–880. https://doi.org/10.1038/s41564-018-0190-y.

Trubl, G., Kimbrel, J.A., Liquet-Gonzalez, J., Nuccio, E.E., Weber, P.K., Pett-Ridge, J., Jansson, J.K., Waldrop, M.P., Blazewicz, S.J., 2021. Active virus-host interactions at sub-freezing temperatures in Arctic peat soil. Microbiome 9, 208. https://doi.org/10.1186/s40168-021-01154-2.

Turetsky, M.R., 2003. The role of bryophytes in carbon and nitrogen cycling. The Bryologist 106, 395–409. https://doi.org/10.1639/05.

Turunen, J., Tomppo, E., Tolonen, K., Reinikainen, A., 2002. Estimating carbon accumulation rates of undrained mires in Finland–application to boreal and subarctic regions. The Holocene 12, 69–80. https://doi.org/10.1191/0959683602hl522rp.

Urbanová, Z., Hájek, T., 2021. Revisiting the concept of 'enzymic latch' on carbon in peatlands. Science of the Total Environment 779, 146384. https://doi.org/10.1016/j.scitotenv.2021.146384.

Verhoeven, J.T.A., Liefveld, W.M., 1997. The ecological significance of organochemical compounds in *Sphagnum*. Acta Botanica Neerlandica 46, 117–130. https://doi.org/10.1111/plb.1997.46.2.117.

Watmough, S., Gilbert-Parkes, S., Basiliko, N., Lamit, L.J., Lilleskov, E.A., Andersen, R., del Aguila-Pasquel, J., Artz, R.E., Benscoter, B.W., Borken, W., Bragazza, L., Brandt, S.M., Bräuer, S.L., Carson, M.A., Chen, X., Chimner, R.A., Clarkson, B.R., Cobb, A.R., Enriquez, A.S., Farmer, J., Grover, S.P., Harvey, C.F., Harris, L.I., Hazard, C., Hoyt, A.M., Hribljan, J., Jauhiainen, J., Juutinen, S., Kane, E.S., Knorr, K.-H., Kolka, R., Könönen, M., Laine, A.M., Larmola, T., Levasseur, P.A., McCalley, C.K., McLaughlin, J., Moore, T.R., Mykytczuk, N., Normand, A.E., Rich, V., Robinson, B., Rupp, D.L., Rutherford, J., Schadt, C.W., Smith, D.S., Spiers, G., Tedersoo, L., Thu, P.Q., Trettin, C.C., Tuittila, E.-S., Turetsky, M., Urbanová, Z., Varner, R.K., Waldrop, M.P., Wang, M., Wang, Z., Warren, M., Wiedermann, M.M., Williams, S.T., Yavitt, J.B., Yu, Z.-G., Zahn, G., 2022. Variation in carbon and nitrogen concentrations among peatland categories at the global scale. PLoS One 17, e0275149. https://doi.org/10.1371/journal.pone.0275149.

Webster, K.L., Bhatti, J.S., Thompson, D.K., Nelson, S.A., Shaw, C.H., Bona, K.A., Hayne, S.L., Kurz, W.A., 2018. Spatially-integrated estimates of net ecosystem exchange and methane fluxes from Canadian peatlands. Carbon Balance and Management 13, 16. https://doi.org/10.1186/s13021-018-0105-5.

Wei, H., Xu, Q., Taylor, L.E., Baker, J.O., Tucker, M.P., Ding, S.-Y., 2009. Natural paradigms of plant cell wall degradation. Current Opinion in Biotechnology 20, 330–338. https://doi.org/10.1016/j.copbio.2009.05.008.

Whang, K.-S., Lee, J.-C., Lee, H.-R., Han, S.-I., Chung, S.-H., 2014. Terriglobus tenax sp. nov., an exopolysaccharide-producing acidobacterium isolated from rhizosphere soil of a medicinal plant. International Journal of Systematic and Evolutionary Microbiology 64, 431–437. https://doi.org/10.1099/ijs.0.053769-0.

Williamson, K.E., Fuhrmann, J.J., Wommack, K.E., Radosevich, M., 2017. Viruses in soil ecosystems: an unknown quantity within an unexplored territory. Annu. Rev. Virol. 4, 201–219. https://doi.org/10.1146/annurev-virology-101416-041639.

Woodcroft, B.J., Singleton, C.M., Boyd, J.A., Evans, P.N., Emerson, J.B., Zayed, A.A.F., Hoelzle, R.D., Lamberton, T.O., McCalley, C.K., Hodgkins, S.B., Wilson, R.M., Purvine, S.O., Nicora, C.D., Li, C., Frolking, S., Chanton, J.P., Crill, P.M., Saleska, S. R., Rich, V.I., Tyson, G.W., 2018. Genome-centric view of carbon processing in thawing permafrost. Nature 560, 49–54. https://doi.org/10.1038/s41586-018-0338-1.

Wu, J., Roulet, N.T., 2014. Climate change reduces the capacity of northern peatlands to absorb the atmospheric carbon dioxide: the different responses of bogs and fens: peatlands switch to C sources by 2100. Global Biogeochemical Cycles 28, 1005–1024. https://doi.org/10.1002/2014GB004845.

Xu, J., Morris, P.J., Liu, J., Holden, J., 2018. PEATMAP: refining estimates of global peatland distribution based on a meta-analysis. Catena 160, 134–140. https://doi.org/10.1016/j.catena.2017.09.010.

Ye, R., Jin, Q., Bohannan, B., Keller, J.K., McAllister, S.A., Bridgham, S.D., 2012. pH controls over anaerobic carbon mineralization, the efficiency of methane production, and methanogenic pathways in peatlands across an ombrotrophic–minerotrophic gradient. Soil Biology and Biochemistry 54, 36–47. https://doi.org/10.1016/j.soilbio.2012.05.015.

Yu, Z., Beilman, D.W., Frolking, S., MacDonald, G.M., Roulet, N.T., Camill, P., Charman, D.J., 2011. Peatlands and their role in the global carbon cycle. Eos Trans. Am. Geophys. Union 92, 97–98. https://doi.org/10.1029/2011EO120001.

Yu, Z., Loisel, J., Brosseau, D.P., Beilman, D.W., Hunt, S.J., 2010. Global peatland dynamics since the last glacial maximum. Geophysical Research Letters 37, L13402. https://doi.org/10.1029/2010GL043584.

Zhang, H., Yohe, T., Huang, L., Entwistle, S., Wu, P., Yang, Z., Busk, P.K., Xu, Y., Yin, Y., 2018. dbCAN2: a meta server for automated carbohydrate-active enzyme annotation. Nucleic Acids Research 46, W95–W101.